Available online at www.sciencedirect.com
ScienceDirect
Progress in Surface Science 82 (2007) 193–223
Progress in SURFACE SCIENCE
www.elsevier.com/locate/progsurf

Review

Theory of two-photon photoemission spectroscopy of surfaces

H. Ueba [a,*], B. Gumhalter [b]

[a] *Department of Electronics, University of Toyama, 930-8555 Toyama, Japan*
[b] *Institute of Physics, HR-10000 Zagreb, Croatia*

Abstract

We review the various theoretical approaches that have recently been developed to interpret the two-photon photoemission (2PPE) spectra from clean and adsorbate-covered metal surfaces. To discuss the most salient features of the 2PPE process in a simple framework we adopt a paradigmatic model system comprising the occupied initial continuum or discrete states, a discrete unoccupied intermediate state, and the continuum of final states above the vacuum level. Starting from this model we introduce quantum-mechanical expressions for the steady state 2PPE transition rates and spectra which enable simple identification of the elementary processes constituting a 2PPE event and the various relaxation and decoherence mechanisms that may affect them and thereby modify the final spectral shapes. On noting the technical difficulties associated with the implementation of the full microscopic description of the time-resolved 2PPE, we review the use of the Optical Bloch Equations (OBE) based on the density matrix method for a phenomenological description of the 2PPE spectra. The OBE pertaining to a three level system are solved to study as how the dephasing times (energy and phase relaxation) of the excited state can be determined from the characteristics of the energy- and time-resolved 2PPE spectra of image potential states at metal surfaces. The results of these modeling procedures also enable us to point out some deficiencies and limitations of the phenomenological approaches based on the OBE in the interpretations of 2PPE experiments. Lastly, we discuss recent attempts to remedy this situation by providing completely microscopic descriptions of dephasing and decay of intermediate states in 2PPE from surface bands in the context of ultrafast carrier dynamics at surfaces.

* Corresponding author. Tel./fax: +81 76 445 6726.
E-mail address: ueba@eng.u-toyama.ac.jp (H. Ueba).

0079-6816/$ - see front matter © 2007 Elsevier Ltd. All rights reserved.
doi:10.1016/j.progsurf.2007.03.002

Keywords: Two-photon photoemission; Pump-probe spectroscopy; Surface states; Image potential states; Adsorbate states; Ultrafast electron dynamics; Relaxation and decoherence; Optical Bloch equations; Density matrix; Quasiparticle evolution; Non-Markovian processes

Contents

1. Introduction

Photoemission spectroscopy has established itself as the most versatile technique for studying the electronic states of solids, surfaces and of adsorbates on solid surfaces [1–4]. The photoemission spectra provide information on the initial density of states below the Fermi level E_F of the studied system from which photoelectrons are excited into the states above the vacuum level E_{vac}. Photoemission may take place either as a result of a single photon absorption process [5–8], provided the photon energy exceeds the work function ϕ of the system, or as a result of absorptions of two photons [9,5,10–12], conveniently termed the pump and probe photons of energy $\hbar\omega_{pu}$ and $\hbar\omega_{pr}$, respectively, under the conditions

$$\hbar\omega_{pu} < \phi \quad \text{and} \quad \hbar\omega_{pu} + \hbar\omega_{pr} > \phi, \tag{1}$$

(hereafter all the energies will be referred to E_F, unless stated otherwise). In the latter process of two-photon-photoemission (2PPE) the first pump photon $\hbar\omega_{pu}$ excites an electron from an occupied state below E_F to an intermediate state between E_F and E_{vac} (including virtual, energy non-conserving transitions). During the survival time in the transiently populated intermediate state this electron can be excited above E_{vac} into the final photoelectron state by absorption of a second probe photon $\hbar\omega_{pr}$. The kinetic energy distribution curve of photoelectrons in the final state gives the 2PPE spectrum.

2PPE spectroscopy combines the advantages of both the traditional one-photon photoemission (1PE) of occupied states and inverse photoemission (IPE) spectroscopy of unoccupied states, thereby allowing a simultaneous detection of occupied and unoccupied excited states in a single experiment and with high energy resolution. With the help of suitable pulsed laser sources, 2PPE spectroscopy provides a unique method for exploring the electronic properties of unoccupied excited states including the image potential states

(IPS) and hot-electron states in metals, as well as the adsorbate excited states on metal surfaces. A natural extension of the energy-resolved 2PPE is the time resolved 2PPE (TR-2PPE) in which the time delay between the pump and probe photons enables the measurement of lifetime of an intermediate state. The performance of TR-2PPE spectroscopy has been greatly enhanced by the advent of ultrafast laser pulses with the duration of several tens of femtoseconds. The last decade has witnessed a rapid progress in the use of TR-2PPE spectroscopy in the measurement of ultrafast excitation and relaxation dynamics of electrons in the femtoseconds time domain, for example of the image potential states (IPS) on metal surfaces.

The goal of this review is to provide a general outline of theoretical foundations of 2PPE spectroscopy with an emphasis on the basic principles of elementary processes in 2PPE from surface states on metal surfaces. Spectroscopic and time-resolved studies of unoccupied surface states by the mid-1990's have been compiled in earlier reviews [4,10]. Although the present review does not intend to duplicate the previous ones, the basic principles of 2PPE spectroscopy and some of the selected materials found in Refs. [4,10] and in this volume are briefly reviewed in order to enable a self-contained discussion of the theory of 2PPE spectroscopy. Among the extensive body of experimental works using TR-2PPE spectroscopy, the topics of hot-electron dynamics in metals are covered in a review by Petek and Ogawa [12], who developed a sophisticated 2PPE technique of interferometric two-pulse correlation for studying the polarization decay (phase relaxation) time of hot electrons in metals. A review of the theoretical treatments of 2PPE from bulk bands has been presented by Timm and Bennemann [13]. Analyses of the various electronic relaxation mechanisms that affect the 2PPE spectra from metal surfaces have been reviewed by Sakaue [14].

This review is organized as follows. In Section 2 elementary processes of 2PPE and the features they induce in the measured spectra are described using a simple model. The emphasis is placed on the conditions under which the intrinsic linewidth of the intermediate state can be deduced from the line-profile analysis of 2PPE spectra obtained from the lifetime measurements. Section 3 is devoted to a comprehensive analysis of both the energy- and time-resolved 2PPE spectra using the phenomenologially parameterized optical Bloch equations (OBE). Invoking the OBE in the analysis of TR-2PPE enables a simple and intuitive treatment of energy (population) relaxation time T_1 and dephasing time T_2 ($1/T_2 = 1/2T_1 + 1/T_2^*$) as separate phenomenological quantities, and to elucidate the importance of introducing a pure dephasing time T_2^* in order to retrieve intermediate state peak(s) in the calculated 2PPE spectra. At this point we also present an analysis of the transient population of the excited state that enables determination of the relaxation time much shorter than the laser pulse duration [15]. A density matrix formulation for a simple three-level system reveals two different paths leading to final photoelectron states (direct two-photon ionization process via non-resonant virtual transition and step-by-step one photon process through a real transition to the intermediate state). Transient response of the 2PPE signal is separated into these two different processes in order to clarify the influence of detuning and pulse duration on the cross-correlation trace of the intermediate state, from which the population relaxation time is estimated. In Section 4 we point out some deficiencies of the phenomenological approaches based on the OBE and discuss recent attempts and progress in providing completely microscopic descriptions of dephasing and decay of intermediate states in 2PPE from surface bands. Summary is presented in Section 5.

2. Elementary processes in 2PPE

A two-photon-photoemission spectrum represents energy distribution curve of the photoelectrons whose number is measured as a function of their kinetic energy and emission angle. The characteristics of 2PPE spectra do not depend only on the electronic properties of the initial and intermediate states but also on the energy and modulation of the applied photon fields. It has been well established that a peak in 2PPE spectrum can be easily assigned to an initial or intermediate state, depending on the peak shift relative to the energies of pump and probe photons, $\hbar\omega_{\mathrm{pu}}$ and $\hbar\omega_{\mathrm{pr}}$, respectively. When a coherent two-photon excitation from an occupied state ϵ_i below E_{F} brings an electron above E_{vac}, the photoelectron kinetic energy ϵ_{p} is given by

$$\epsilon_{\mathrm{p}} = \hbar\omega_{\mathrm{pu}} + \hbar\omega_{\mathrm{pr}} + \epsilon_i. \tag{2}$$

When the 2PPE is due to two independent processes, the transient population in an intermediate state ϵ_j caused by $\hbar\omega_{\mathrm{pu}}$ and a subsequent excitation above E_{vac} by $\hbar\omega_{\mathrm{pr}}$, the photoelectron energy varies with $\hbar\omega_{\mathrm{pr}}$ as

$$\epsilon_{\mathrm{p}} = \hbar\omega_{\mathrm{pr}} + \epsilon_j. \tag{3}$$

Here it should be noted that simple relation (3) holds only in the absence of dispersion of the relevant electronic states with the component of the electron wave vector parallel to the surface [16,17].

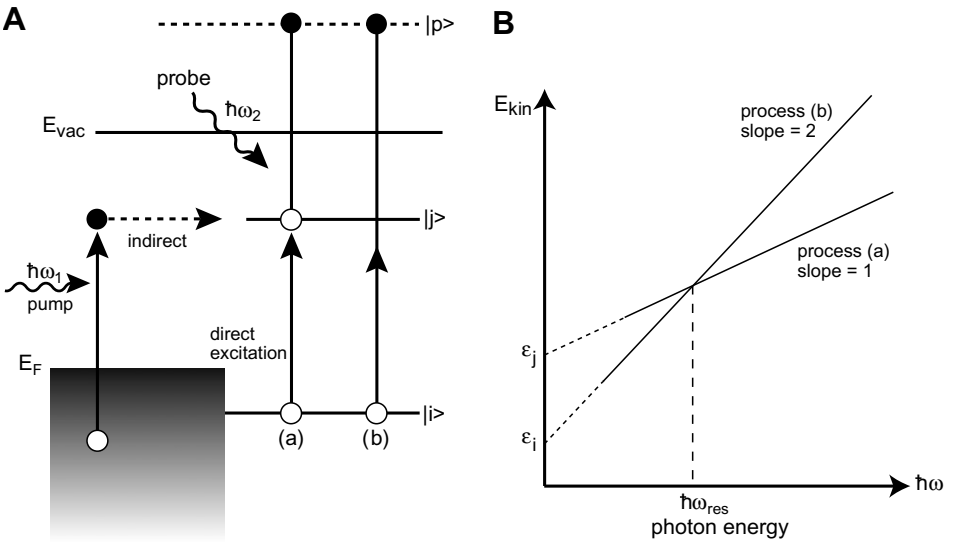

Fig. 1. (A) Elementary excitation processes in two-photon photoemission. When a discrete surface state and a continuum of the substrate are available for initial states $|i\rangle$, there are two paths leading to a temporal population of the intermediate state $|j\rangle$. One is direct excitation leading to *step-by-step* one-photon transition and another is indirect process via scattering of photo-excited electron from a continuum. If there is no surface state like on Cu(100), only the latter non-resonant process is possible. There are two paths leading to a final photoelectron state $|p\rangle$ via (a) *step-by-step* one-photon process and (b) direct two-photon ionization process from $|i\rangle$. (B) $\hbar\omega$ dependence of the photoelectron kinetic energy, and $\hbar\omega_{\mathrm{res}} = \epsilon_j - \epsilon_i$ is a resonant excitation leading to a single narrower peak, as described in the text.

Although the peak shift upon variation of the photon energy allows one to identify a single peak as being due either to an initial state, an intermediate state or a final state, relatively little is known about the elementary excitation mechanisms. Fig. 1A schematically illustrates the possible excitation pathways leading to the final photoelectron states. This energy diagram includes a bulk continuum and a localized surface state (SS) below E_F of the metal, and an unoccupied image potential state (IPS) between E_F and E_{vac}. Fig. 1B depicts ϵ_p as a function of the excitation energy $\hbar\omega = \hbar\omega_{pu} = \hbar\omega_{pr}$. The incoherent step-by-step single photon process (a) gives a slope = 1, while the coherent two-photon process (b) gives a slope = 2. Their extrapolations to $\hbar\omega \to 0$ determine ϵ_i and ϵ_j. At resonant excitation ($\hbar\omega = \epsilon_j - \epsilon_i$), two peaks arising from the initially occupied SS and unoccupied intermediate states merge into a single narrow peak. This diagram illustrates the simplest version of the system with occupied surface and unoccupied image potential states, typical of, e.g., Cu(1 1 1) and Ag(1 1 1) surfaces. In this case there are two channels for populating the IPS. One is a direct excitation from the SS. At the same time, even for pump photon energies below or above the direct transition, the IPS can be also populated via the excitation of bulk electrons to the IPS at $k_{\|} \neq 0$ followed by intraband relaxation leading to a population at $k_{\|} = 0$. This excitation mechanism involving electronic dephasing has been suggested in order to establish a consistent analysis of both the energy-, and time-resolved 2PPE spectra from Cu(1 1 1) surface [18].

Fig. 2 schematically illustrates the band structure of a Cu(1 1 1) at $k_{\|} = 0$, and the wave function for the surface state ($n = 0$) and the first IPS ($n = 1$), whose penetration into the

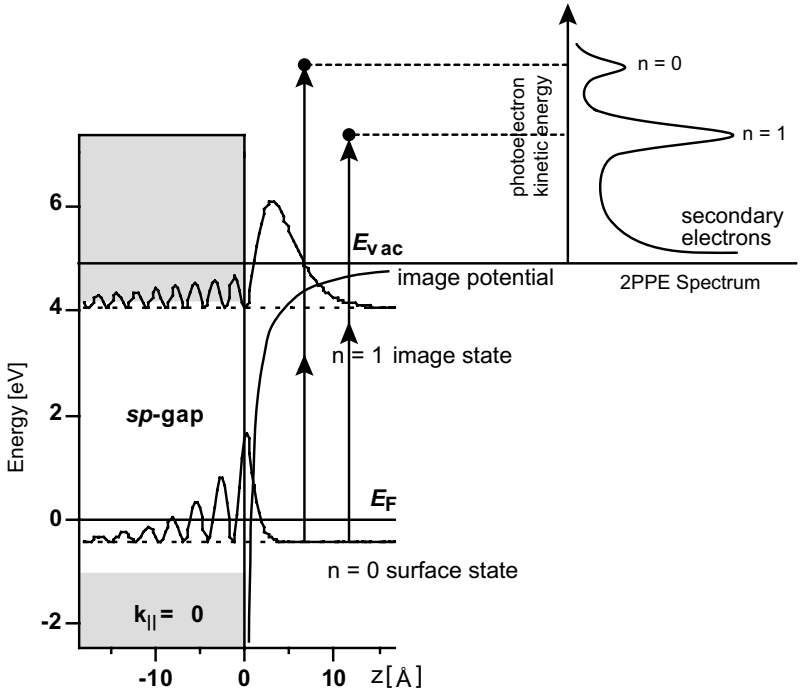

Fig. 2. Band structure of Cu(1 1 1) at $k_{\|} = 0$ and the wave function of an occupied surface state and the first image potential state. A typical 2PPE spectrum is also shown (Courtesy of M. Wolf).

bulk depends on the position relative to the surface projected sp-bulk band gap. A typical 2PPE spectrum including photo-excited secondary electron emission is also shown.

In the case of (1 0 0) surfaces of Au and Cu that have no occupied SS at $k_{\|} = 0$, an electron is excited from a continuum of initial bulk states below E_F to IPS. This implies indirect and non-resonant electron excitation into the IPS via scattering of hot-electrons excited from the bulk continuum. The direct and indirect excitation mechanisms differ in the role of coherence and manifest themselves both in the time-resolved 2PPE spectrum and the polarization dependence of the 2PPE intensity [19].

A similar scenario can be also applied to an adsorbate-metal system, e.g. carbon monoxide (CO) on metal surfaces, in which the $2\pi^*$-derived level serves as an intermediate state in the 2PPE process. Among the many adsorbate–metal systems, chemisorption of CO molecules on single crystal Cu surfaces is a prototype system to which various spectroscopic techniques have been employed to investigate their electronic and vibrational properties [20,21]. In particular, the lifetime of the normally unoccupied $2\pi^*$ derived states is of primary interest for gaining a deeper insight in photochemical surface reactions [22], and the time-resolved 2PPE spectroscopy has been successfully employed to estimate T_1 of the $2\pi^*$ state of CO on Cu(1 1 1) [23,24]. Since the highest occupied state deriving from the $5\sigma/1\pi$ orbitals of chemisorbed CO is located far below E_F, the $2\pi^*$ state at about 3.4 eV above E_F can be only populated by a photo-excited electron from the substrate continuum via indirect processes. In fact, temporal formation of the negative ion by population of the $2\pi^*$-derived state through hot-electron scattering has been proposed to be a trigger of the various photo-driven surface reactions such as desorption [25,26]. A manipulation of individual CO molecules on Cu(1 1 1) by a scanning tunneling microscope (STM) is also one of the most exciting results in the field of surface science and is found to be induced by the transient population of the CO $2\pi^*$ level by electrons tunneling from the STM tip [23].

2.1. Model description of 2PPE spectra

The elementary processes and the spectral features of 2PPE are studied using a model Hamiltonian:

$$H = \sum_i \epsilon_i n_i + \epsilon_j n_j + H^j_{\mathrm{int}} + \sum_p \epsilon_{\mathrm{p}} n_{\mathrm{p}} + H^{\mathrm{ph}}_{\mathrm{int}}, \tag{4}$$

where $\epsilon_{i(j,p)}$ is the energy of the initial state $|i>$, intermediate state $|j>$ and the continuum of final photoelectron state $|p>$, respectively, and $n = c^\dagger c$ denotes the number operator of each state. Here $|i>$ is assumed to range over the discrete SS and the continuum of states $|k>$ below the Fermi level. The effect of band broadening of the intermediate states will be discussed in the next section. The term H^j_{int} is the interaction Hamiltonian responsible for the relaxation of the photo-excited electrons and holes in the intermediate states.

The optical perturbation of the system due to its interaction with a photon field is given by

$$H^{\mathrm{ph}}_{\mathrm{int}}(t) = -\vec{\mu}\cdot\vec{E}(t), \quad \vec{E}(t) = \vec{E}_{\mathrm{pu}}(t)\mathrm{e}^{-\mathrm{i}\hbar\omega_{\mathrm{pu}}t} + \vec{E}_{\mathrm{pr}}(t)\mathrm{e}^{-\mathrm{i}\hbar\omega_{\mathrm{pr}}t} + h.c., \tag{5}$$

where $\vec{\mu}$ is the dipole operator. In a conventional 2PPE spectroscopy, the energy-resolved spectrum is observed with a nanosecond laser source for the sake of high-energy resolution. Since in this case the pulse duration is sufficiently longer than the time scales typical of the relaxation dynamics of the intermediate state probed by 2PPE, the time envelope of

the photon fields $E_{\mathrm{pu,\,pr}}(t)$ can be taken as constant (continuous light beams). Then the interaction Hamiltonian $H_{\mathrm{int}}^{\mathrm{ph}} = H_{\mathrm{pu}}$ (between $|i\rangle$ and $|j\rangle$) + H_{pr} (between $|j\rangle$ and $|p\rangle$) is expressed as

$$H_{\mathrm{pu}} = \sum_i M_{ji} \mathrm{e}^{-\mathrm{i}\hbar\omega_{\mathrm{pu}}t} c_j^+ c_i + h.c., \quad H_{\mathrm{pr}} = \sum_p M_{pj} \mathrm{e}^{-\mathrm{i}\hbar\omega_{\mathrm{pr}}t} c_p^+ c_j + h.c., \tag{6}$$

where $M_{ij} = \vec{\mu}_{ij} \cdot \vec{E}_{\mathrm{pu}}$ and $M_{pj} = \vec{\mu}_{pj} \cdot \vec{E}_{\mathrm{pr}}$ represent the dipole transition matrix elements between $|i\rangle$ and $|j\rangle$, and $|j\rangle$ and $|p\rangle$, respectively. Further simplification is made that all the transition matrix elements are assumed to be constant, viz., $M_{ij} = M_{\mathrm{pu}}$ and $M_{pj} = M_{\mathrm{pr}}$.

Then, in the rotating wave approximation the 2PPE spectrum assumes the form

$$P(\hbar\omega_{\mathrm{pu}}, \hbar\omega_{\mathrm{pr}}; \epsilon) = \sum_p \left| 2\pi \sum_i M_{pj} \frac{1}{\hbar\omega_{\mathrm{pu}} + \epsilon_i - \epsilon_j} M_{ji} \delta(\hbar\omega_{\mathrm{pp}} + \epsilon_i - \epsilon_p) \right|^2 \delta(\epsilon - \epsilon_p), \tag{7}$$

where $\hbar\omega_{pp} = \hbar\omega_{\mathrm{pr}} + \hbar\omega_{\mathrm{pr}}$. Hereafter the constant factors $|M_{\mathrm{pu}}|^2 |M_{\mathrm{pr}}|^2$ will be omitted. Using the resolvent expansion method and introducing the Lorentzian substrate density of states $\rho_i(\epsilon) = (\gamma_i/\pi)/[(\epsilon - \epsilon_i)^2 + \gamma_i^2]$ of intrinsic halfwidth γ_i for the initial state, one can obtain for the spectral intensity in Eq. (7)

$$P(\hbar\omega_{\mathrm{pu}}, \hbar\omega_{\mathrm{pr}}; \epsilon_p) = \frac{2}{[(\epsilon_p - \hbar\omega_{\mathrm{pp}} - \epsilon_i)^2 + \gamma_i^2]} \frac{1}{[(\epsilon_p - \hbar\omega_{\mathrm{pr}} - \epsilon_j)^2 + \gamma_j^2]}, \tag{8}$$

where the linewidth γ_j introduced to describe the effect of H_{int}^j is implicitly assumed to contain both the energy (population) relaxation time T_1 and the so-called pure dephasing time T_2^*, i.e., $\gamma_j = 1/T_2 = 1/2T_1 + 1/T_2^*$. The 2PPE spectrum exhibits two peaks whose energies are given by Eqs. (2) and (3). This is a consequence of the requirement of total energy conservation in a 2PPE event. It is not satisfied at off-resonant pump excitation to a non-fixed virtual state. Because of the presence of the continuum photoelectron states $|p\rangle$, the 2PPE probability reaches maximum at $\hbar\omega_{\mathrm{pu}}$ in order to satisfy the energy conservation of the whole 2PPE process in the final state. However, this is not the case with *one-photon* photoemission from the intermediate state, in which the energy conservation is satisfied in each *step-by-step* photo-excitation process.

An important implication of expression (8) relates to the determination of intrinsic linewidth γ_j of the intermediate state peak which has here been introduced as a phenomenological parameter. In the case of a narrow SS-band that serves as the initial state and the pump excitation set far from the resonance, the 2PPE spectrum exhibits well-separated two Lorentzians whose linewidths can be taken as the intrinsic ones after being convoluted with the instrumental broadening. On approaching the resonant excitation at $\hbar\omega_{\mathrm{pu}} = \hbar\omega_j - \hbar\omega_i$, the tail of the growing peak of the initial state contributes to the intensity of the intermediate state peak. The 2PPE spectrum at resonance, $P(\hbar\omega_{\mathrm{pu}} = \epsilon_j - \epsilon_i, \hbar\omega_{pr};\ \epsilon_p)$, shows a single enhanced peak with the full width at half maximum (FWHM) given approximately by $\Gamma_{\mathrm{res}} = 2\gamma_i\gamma_j/(\gamma_i^2 + \gamma_j^2)^{1/2}$. This means that for systems in which the initial state has a width comparable to or narrower than the intermediate state, i.e., $\gamma_i < \gamma_j$, the intrinsic width of the intermediate state cannot be determined from the observed linewidth of the 2PPE spectrum [27] because in this case $\Gamma_{\mathrm{res}} \to 2\gamma_i$. In the opposite limit $\gamma_i \gg \gamma_j$, Γ_{res} approaches the intrinsic linewidth $2\gamma_j$ of the intermediate state. For $2\gamma_j > \Gamma_{\mathrm{res}}$, a narrowing occurs at resonance, as has indeed been observed in many 2PPE spectra [19,28,29]. When a smooth continuum below E_{F} serves as the initial state

from which electrons are excited into the intermediate state by non-resonant excitation, the first factor of (8) is replaced by a constant initial density of states ρ_i. In this case the 2PPE spectrum exhibits a single peak due to "one-photon" photoemission from the intermediate state, so that neither the resonance enhancement of the 2PPE intensity nor the narrowing of the linewidth occur.

2.2. Application of the model to prototype systems

With the theoretical prerequisites formulated in the preceding subsection we may take a look at the results of experiments which have focused on measuring the intrinsic linewidths in 2PPE spectra. In the early 1990's, a series of high-resolution bichromatic 2PPE measurements of the linewidths of IPS on several clean metal surfaces have been reported [30,31]. Fig. 3 compares the 2PPE spectra for the (100) and (111) surfaces of Cu [10]. A clean Cu(111) surface has the occupied SS and the first IPS at 0.38 eV below and 4.1 eV above E_F, respectively. The spectrum of the (111) face was observed at resonant excitation of $\hbar\omega_{pu} = 4.48$ eV, while no resonance occurs for the (100) surface. One can easily notice a striking difference of the linewidth between the two faces of Cu. From a line-profile analysis, the linewidths of 16 meV and 85 meV were obtained for Cu(111) and Cu(100), respectively. Schuppler et al. [31] argued that linewidths determined by the line-shape analysis do not necessarily correspond to the lifetimes of the IPS, and that the broadening of initial SS may also be involved. Following a simple second order perturbation analysis [1] combined with a separate measurement of the intrinsic SS width on Cu(111) by one-photon photoemission, they concluded that after the first excitation step the electrons loose information on their origin from the initial state and hence the measured Lorentzian width is just the width of the intermediate state. As described above, however, this is not a proper way to deduce the intrinsic linewidth from the line-profile

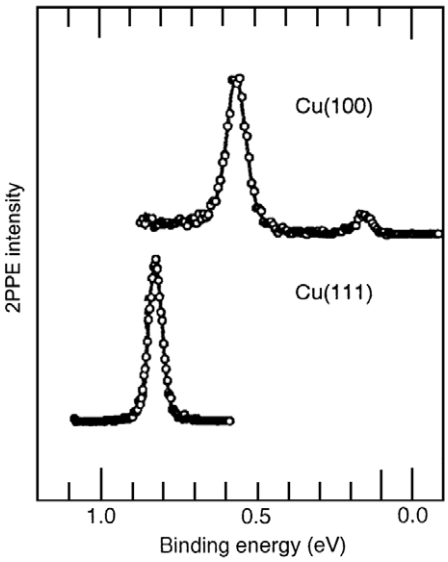

Fig. 3. Two-photon photoemission spectra for Cu(111) and Cu(100) observed at on-and off-resonance excitation, respectively (from Ref. [10]).

analysis of 2PPE spectra. The linewidth of 16 ± 4 meV corresponds to the dephasing time of about 42 fs, which is several times longer than T_1 determined from the time-resolved 2PPE experiments [15,18,32].

The intrinsic linewidth of 21 ± 4 meV has been obtained for the $n = 1$ IPS on a Ag(1 0 0) surface [33]. If we assume, for the moment, that this linewidth is predominantly governed by the population relaxation, this is converted into $T_1 = 26$–39 fs. One of the recent time-resolved studies of IPS on Ag(1 0 0) and Cu(1 0 0) has reported much longer $T_1 = 55 \pm 5$ fs [34] for the $n = 1$ IPS on Ag(1 0 0), which contributes 11–13 meV to the linewidth. The most plausible origin of the difference between the intrinsic half width ($T_2 = 62.5$ fs) and T_1 is ascribed to the pure dephasing time T_2^*. Using the analysis based on the density matrix formalism (see Section 3), $T_2^* = 140$ fs was estimated for the $n = 1$ IPS on Ag(1 0 0).

In spite of the simplicity of the present model these results demonstrate a condition under which the intrinsic linewidth (which can be compared to the time-resolved studies) can be reliably deduced from the lineshape analysis of the energy-resolved 2PPE spectrum. For a continuum initial state, the measured linewidth directly corresponds to the intrinsic linewidth of the intermediate state. On the other hand, for a narrow initial state it can only be estimated at off-resonant excitation producing a well separated two peak structure. In this respect the excitation spectrum, i.e., the evolution of 2PPE spectrum with $\hbar\omega_{pu}$, provides the most reliable determination of the intrinsic linewidth of the intermediate state peak.

Experimental work along this line has been reported by Wallauer and Fauster [29]. Fig. 4 shows the evolution of the 2PPE spectra of a Cu(1 1 1) surface for various $\hbar\omega_{pu}$. In qualitative agreement with (8) the 2PPE spectrum at resonant excitation exhibits the narrowest linewidth and two peaks in the spectra for $\hbar\omega_{pu} = 535$ and 585 nm show broader widths than observed at resonance. The model of the product of two Lorentzians

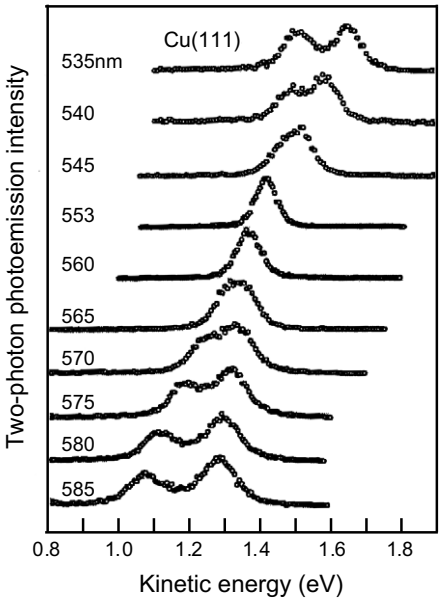

Fig. 4. Evolution of two-photon photoemission spectra of Cu(1 1 1) for different wavelengths of the pump photon (from Ref. [29]).

plus some contribution from non-$\vec{k}_{\parallel}$ conserving excitations to the IPS was employed to reproduce the complete series of the 2PPE spectra in terms of the intrinsic linewidths of 65 ± 15 meV for the SS and 85 ± 10 meV for the $n = 1$ IPS.

These widths should be compared with the TR-2PPE measurement of the lifetime T_1 of the IPS on a Cu(1 1 1) surface. The obtained width of the IPS corresponds to a dephasing time of $T_2 = 15$ fs. Many experimental results have been reported for the T_1 determination of the IPS ($n = 1$) on a Cu(1 1 1) surface [18,32]. The most refined T_1 of the $n = 1$ IPS on a Cu(1 1 1) surface is 18 ± 5 fs [32] (contributing 37 meV to the linewidth). If we take $T_2 = 15$ fs and $T_1 = 18$ fs, the pure dephasing time $T_2^* = 27$ fs is obtained.

The line-profile analyses of the 2PPE spectra suggest a crucial role played by pure dephasing in the excitation and relaxation dynamics of IPS's on metal surfaces. At the early stage of 2PPE studies, the importance of pure dephasing was invoked in order to account for the discrepancy between the observed linewidth and T_1 determined by TR-2PPE and/or to reproduce both the initial and the intermediate state lineshapes with a single set of parameters including pure dephasing. While a large body of TR-2PPE studies have been directed to determine T_1, a relatively little was known about a pure dephasing T_2^* in interferometric time-resolved 2PPE [36], quantum-beat 2PPE [35,37–39] and the temperature dependence of the lifetime/linewidth of the SS and IPS on Cu(1 0 0) and Cu(1 1 1) [40].

Here a connection can be made with the studies of vibrational relaxation of adsorbates on solid surfaces [41]. Among several pump-probe surface vibrational spectroscopies, the so-called *free induction decay-sum frequency generation* (FID-SFG) provides a unique tool for measuring the total dephasing time T_2. Guyot-Sionnest [42] was the first to measure T_2 of the Si–H stretching vibration on H-terminated Si(1 1 1) surface. Since the T_1 relaxation process was found to give a negligible contribution to the observed linewidth of the infrared absorption spectrum, it was concluded that pure dephasing and inhomogeneous broadening (quantitatively estimated by vibrational photon echo technique) were mostly responsible for the observed linewidth. A similar T_2 determination was also carried out for the C–O stretching mode of CO on Cu(1 1 1) by Owrutsky et al. [43]. In that experiment the temporal evolution of vibrational coherence generated by using a 380 fs IR pulse was monitored by up-converting the decaying polarization with a time-delayed 280 fs visible pulse. It was found that the decay could be well-fitted by a single exponential, thereby allowing to estimate $T_2 = 2.0 \pm 0.3$ ps. It took almost ten years to report the next FID-SFG experiment, which was employed to study the vibrational relaxation of the C–O stretching mode of CO adsorbed on Ru(0 0 1) surface during dynamical processes of CO desorption [44]. In this study an IR pulse with a duration $t_p = 150$ fs followed by a time-delayed visible pulse of 110 fs was used to observe the transient response of the FID-SFG, which exhibited an exponential decay with a time constant $T_2 = 1.16$ ps ($\gg t_p$). In these time-resolved studies of vibrational relaxation the pulse duration was much shorter than both the population and dephasing time of the vibrational mode of interest. Accordingly, a precise determination of the relaxation time could easily be made from the decaying slope. By contrast, such a fortitous situation is not the case in ultrafast electronic relaxation at metal surfaces.

3. Time-resolved two-photon photoemission

Recent advances in the generation of ultrafast laser pulses have made possible direct access to dynamical electronic properties in the real time domain down to few femtosec-

onds. A rapidly growing activity in the study of ultrafast dynamics of electronic excitation and relaxation in the bulk and at metal surfaces has been compiled in recent reviews [12,45] and a special issue of Chemical Physics [46]. An introduction to principles and experiments of TR-2PPE including historical overviews of the development in comparison with other techniques is presented in this volume. The present section focuses on the fundamental issues associated with the theoretical treatments of such ultrafast electron dynamics.

We first briefly discuss the physics of basic relaxation processes encountered in TR-2PPE from image potential states at metal surfaces. These states are expected to have much longer lifetimes than the electronic excitations in the bulk because of their localization in front of a surface where the coupling to bulk excitations is relatively weak. Hence, the TR-2PPE spectroscopy offers itself as an ideal tool for monitoring femtosecond relaxation dynamics of image potential states. Nevertheless, as substantial changes of the IPS population may occur on the time scale of the excitation pulse duration t_p, the analysis of the transient 2PPE response involving electrons excited in IPS is not simple.

The key relationship that governs the physics underlying TR-2PPE is the relative time scale among T_1, T_2 and t_p. It is well known in the context of quantum optics [47,48] and ultrashort laser pulse phenomena [49] that in the case $t_p \gg T_2$ there is no coherent superposition of the polarization and electromagnetic field oscillations. Then the memory of the medium is kept only through the change of the population. This is the case where the rate equation approach (no coherence effect) is appropriate for describing the temporal response of the excited population. In this treatment the temporal change of the material system occurring within the interval T_2 is averaged so that only the asymptotic dynamical response beyond the time scale of T_2 is taken into consideration.

On the other hand, in the case $t_p < T_2$, namely when the exciting pulse duration becomes comparable with or even shorter than the phase relaxation time of the excited medium and in the presence of pump and probe overlap during the dynamical change of photo-induced polarization, a model including *coherent interaction* between the photon field and transition dipole moment is required to describe the temporal response of the system. This is accomplished by the Liouville–von Neumann equation describing the temporal evolution of the density matrix ρ of the interacting system:

$$\frac{\mathrm{d}}{\mathrm{d}t}\rho = -i[H_0 + H^c_{\mathrm{int}}, \rho] - i[H^r_{\mathrm{int}}, \rho], \tag{9}$$

where H_0 is the unperturbed Hamiltonian of the electronic system, H^c_{int} is the coherent interaction with the electromagnetic field and H^r_{int} is a random perturbation that acts on the electronic system and is responsible for the relaxation of the excited medium through the coupling with a heatbath.

Eq. (9) is exact and is equivalent to the Schrödinger equation of the studied many-particle system. Within the Markovian approximation, in the regime where a correlation time τ_c of the random force H^r_{int} is short enough compared to the duration of interaction with the photon pulse, the second term on the right-hand-side (RHS) of (9) gives rise to a dissipative contribution to the density matrix which, in this regime, can be approximated in terms of a relaxation time describing the asymptotic evolution of the system. *Relaxation time* can be phenomenologically introduced in the form of the so-called optical Bloch

equations (OBE) for the density matrix, in analogy to the Bloch equations in nuclear magnetic resonance. The matrix elements of the OBE take a general form

$$\frac{\mathrm{d}}{\mathrm{d}t}\rho_{nn} = -i\sum_k \left(H^c_{nk}\rho_{kn} - \rho_{nk}H^c_{kn}\right) - \sum_{k\neq n}\gamma_{nk}(\rho_{nn} - \rho_{kk}), \tag{10}$$

$$\frac{\mathrm{d}}{\mathrm{d}t}\rho_{nm} = -i(\hbar\omega - \hbar\omega_n + \hbar\omega_m) - i\sum_k \left(H^c_{nk}\rho_{km} - \rho_{nk}H^c_{km}\right) - \Gamma_{nm}\rho_{nm}. \tag{11}$$

The diagonal matrix elements ρ_{nn} give the time-dependent population of the state $|n\rangle$ with a population and depopulation rate $\gamma_{nk}(\equiv\gamma_{kn})$. The off-diagonal elements ρ_{nm} represent the optically induced phase coherence between two states $|n\rangle$ and $|m\rangle$, and

$$\Gamma_{nm} = \frac{1}{T_2^{nm}} = \frac{1}{2}\left(\frac{1}{T_1^n} + \frac{1}{T_1^m}\right) + \left(\frac{1}{T_2^{*n}} + \frac{1}{T_2^{*m}}\right), \tag{12}$$

represents the coherence decay (dephasing) during transitions between two states, and T_2^* is the *pure dephasing* time. The phenomenological introduction of the latter compensates for the loss of some interference effects in going from Eq. (9) to Eqs. (10) and (11).

3.1. Energy- and time-resolved 2PPE spectra

The OBE for the density matrix as given by Eqs. (10) and (11) represent a set of coupled differential equations that in the general multilevel case can be solved only numerically. A simplification arises in the case of few level model systems with simple forms of electron–photon field interactions. So far all the detailed analyses of TR-2PPE experiments for a wide variety of electronic relaxation dynamics in metals and at surfaces have been made by resorting to the OBE for a three-level system represented by the initial state $|i\rangle$, intermediate state $|j\rangle$ and final photoelectron state $|p\rangle$ partaking in the 2PPE process. The density matrix describing temporal evolution of populations and polarization in such a system is represented as

$$\rho(t) = \begin{pmatrix} \rho_{ii} & \rho_{ij} & \rho_{ip} \\ \rho_{ji} & \rho_{jj} & \rho_{jp} \\ \rho_{pi} & \rho_{pj} & \rho_{pp} \end{pmatrix}. \tag{13}$$

There are two excitation paths (a) and (b) to reach the final photoelectron state ρ_{pp} from the initial state ρ_{ii}, as depicted in Fig. 1. One is the *step-by-step* one-photon process through the intermediate state: (a) $\rho_{ii} \to \rho_{ij} \to \rho_{jj} \to \rho_{jp} \to \rho_{pp}$ (plus their complex conjugates). The intermediate state population ρ_{jj} is created on the way from $|i\rangle$ to $|p\rangle$, so that this process produces the intermediate state peak in the 2PPE spectrum and delivers information on the population relaxation when a time delay is introduced between pump and probe pulses. Another process is a two-photon ionization process through a virtual transition in which a two-quantum coherence ρ_{pi} is created: (b) $\rho_{ii} \to \rho_{ij} \to \rho_{ip} \to \rho_{jp} \to \rho_{pp}$ (plus their complex conjugates). This process gives not only the initial state peak in the presence of the occupied surface state, but also contributes to the temporal population in the intermediate state and therefore is of special importance in the analysis of both the energy- and time-resolved 2PPE spectra.

3.2. Energy-resolved 2PPE spectra

In order to study the above described two different processes, the energy-resolved 2PPE spectrum for the continuous photon field is calculated by means of perturbation expansion up to the fourth order in the applied electric field $E(t)$. From (12) we introduce a dephasing time associated with $|i> \rightarrow |j>$ transition by

$$\frac{1}{T_2^{ij}} = \frac{1}{2}\left(\frac{1}{T_1^i} + \frac{1}{T_1^j}\right) + \Gamma_{ij}^* \tag{14}$$

where $\Gamma_{ij}^* = \Gamma_i^* + \Gamma_j^*$ is the so-called pure dephasing rate which gives rise to a decay of the coherence between the levels $|i>$ and $|j>$. The following assumptions are made for T_2^{ij} of the three-level system; (1) neglect of the energy relaxation and pure-dephasing in the final state, (2) energy relaxation appears only in the intermediate state. This leads to a relation $1/T_2^{ei} + 1/T_2^{ip}$, where $1/T_2^{jp} = 1/2T_1^e + \Gamma_e^* (\equiv 1/T_2^e$ is the total dephasing rate in the intermediate state) and $1/T_2^{pi} = \Gamma_i^*$.

It is convenient to introduce a single photon lineshape function for the $|i> \rightarrow |j>$ transition, $I_{ij}(\hbar\omega) = (\hbar\omega - \epsilon_{ij} - i/T_2^{ij})^{-1}$. Then, the steady state 2PPE spectrum is written in terms of $I_{ij}(\hbar\omega)$ as

$$P(\hbar\omega_{\mathrm{pu}}, \hbar\omega_{\mathrm{pr}}; \epsilon) = 2T_1 \mathrm{Im}[I_{ji}(\hbar\omega_{\mathrm{pu}})] \cdot \mathrm{Im}[I_{pj}(\hbar\omega_{\mathrm{pr}})] - \mathrm{Im}\left[I_{ji}(\hbar\omega_{\mathrm{pu}}) I_{pj}(\hbar\omega_{\mathrm{pr}}) I_{pi}(\hbar\omega_{pp})\right], \tag{15}$$

where the first term proportional to T_1 represents a step-by-step *incoherent* process (a), while the second term corresponds to a direct *coherent* two-photon ionization process (b). The formal structure of (15) is identical to that derived within the factorization approximation in correlation function theory of coherent two-photon processes [51]. Here it should be noted that the second term contains the same one-photon process $I_{pj}(\hbar\omega_{\mathrm{pr}})$ as the first term. This is a clear indication that the intermediate state can also be populated via the non-resonant virtual excitation (process (b) in Fig. 1).

It is a straightforward calculation to obtain

$$P(\hbar\omega_{\mathrm{pu}}, \hbar\omega_{\mathrm{pr}}; \epsilon_{\mathrm{p}}) = \frac{1}{\left(\hbar\omega_{\mathrm{pr}} + \epsilon_j - \epsilon_{\mathrm{p}}\right)^2 + \left(1/T_2^j\right)^2} \times \left[\frac{\Gamma_i^*}{\left(\hbar\omega_{pp} + \epsilon_i - \epsilon_{\mathrm{p}}\right)^2 + \Gamma_i^{*2}} + 2T_1\Gamma_j^* \frac{1/T_2^{ji}}{\left(\hbar\omega_{\mathrm{pu}} + \epsilon_i - \epsilon_j\right)^2 + \left(1/T_2^{ji}\right)^2}\right]. \tag{16}$$

The first term on the RHS of (16) that comes from the process (b) is the same as expression (8). The second term is due to the process (a) and (b). In the analysis of 2PPE spectra from Cu(1 1 1) surface using (8), Wallauer and Fauster [29] had to introduce an additional Lorentzian contribution to the $n = 1$ IPS. As a possible origin of the additional intensity it has been speculated that excitation of electrons to the IPS at $k_{\|} \neq 0$ followed by intraband relaxation due to scattering by surface defects leads to a population at $k_{\|} = 0$. Expression (16) seems to support another excitation mechanism associated with rapid dephasing of hot-electrons that may give rise to the appearance of intermediate state peak [18]. If there is no pure dephasing in the initial and intermediate states, i.e., $\Gamma_i^* = \Gamma_j^* = 0$, but for a finite pure-dephasing Γ_p^* in the final state, the 2PPE spectrum only shows the initial state peak

[19]. Eq. (16) demonstrates the necessity of introducing pure-dephasing in the initial and intermediate state for the appearance of the intermediate state peak. According to the proposal of the importance of pure-dephasing [15,32], the phase-breaking scatterings during excitation destroy the coherence and generate an incoherent population in the IPS. This may explain why the IPS can be observed at photon energies far away from the resonance.

Fig. 5 shows the evolution of 2PPE spectra as a function of $\hbar\omega_{\rm pu}$ below and above the resonant excitation at $\hbar\omega_{\rm pu} = \hbar\omega_j - \hbar\omega_i$ for $\hbar\omega_{\rm pr} = 2.5$ eV. A set of parameters $\epsilon_i = -0.5$ eV, $\epsilon_j = 4.0$ eV, $T_1 = 20$ fs, $T_2^i = 15$ fs, $T_2 = 50$ fs, and $\phi = 5.0$ eV roughly correspond to a Cu(1 1 1) surface [19]. The spectra show two peaks due to the occupied initial state and the unoccupied excited state. The intermediate excited state peak remains at 6.5 eV, while the initial state peak shifts with $\omega_{\rm pu}$. At resonant excitation $\hbar\omega = 4.5$ eV, the two peaks merge into a single peak showing a linewidth narrowing and enhancement [11]. This indicates that the intrinsic linewidth of the intermediate peak can not be measured in the case of near resonant excitation from the discrete initial state. This also implies that the TR-2PPE experiments carried out to deduce T_1 of the intermediate state from the cross-correlation trace should be performed under non-resonant excitation condition.

When the excitation is far from the resonance condition, i.e., $|\omega_{\rm pu} - \epsilon_{ji}| \gg 1/T_2^{ji}$, expression (16) can be approximated as

$$P(\hbar\omega_{\rm pu}, \hbar\omega_{\rm pr}; \epsilon) \simeq \frac{2T_1\Gamma_j^*/T_2^j}{(\hbar\omega_{\rm pr} + \epsilon_j - \epsilon)^2 + (1/T_2^j)^2} + \frac{1/T_2^i}{(\hbar\omega_{\rm pp} + \epsilon_i - \epsilon)^2 + (1/T_2^i)^2} \tag{17}$$

so that the 2PPE spectrum consists of separated initial and intermediate state peaks. This allows one to determine the intrinsic linewidth (inverse of the total dephasing time).

When electrons are excited from the continuum, the 2PPE spectrum exhibits only the intermediate state peak superimposed on a smooth varying background associated with the 2PPE process from the continuum. In this case no pure-dephasing is necessary for the appearance of the intermediate state peak [19]. It is also noted that no resonance enhancement occurs in the intermediate state peak. This is the case of Cu(100) and

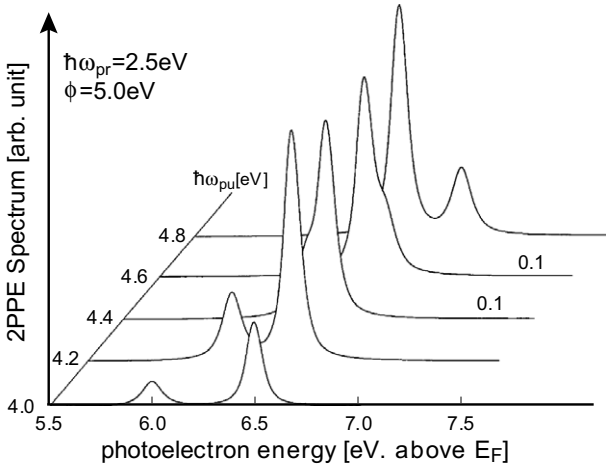

Fig. 5. Evolution of 2PPE spectra as a function of $\hbar\omega_{\rm pu}$, where $\hbar\omega_{\rm pr} = 2.5$ eV is fixed (from Ref. [55]). See the text for the parameters used.

Ag(1 0 0) in which the intermediate state is populated in the process of coherent excitation from the continuum, and the linewidth of the 2PPE spectrum determines T_2 of the intermediate state.

3.3. Time-resolved 2PPE spectra

The first series of the TR-2PPE measurements of T_1 of IPS on Ag(1 0 0) and Ag(1 1 1) were performed by Schoenlein et al. [50]. They observed a distinct asymmetry in the cross-correlation trace (defined as the 2PPE intensity at fixed kinetic energy of photoelectrons emitted from the IPS as a function of pump-probe delay time t_d), whose maximum was shifted from $t_d = 0$. They described the cross-correlation trace by $A(t_d)\exp(-t_d/T_1)$, where $A(t_d)$ is a pump-probe cross-correlation. For the $n = 1$ IPS on a Ag(1 0 0), T_1 was estimated to be 25 ± 10 fs, which is *shorter* than the pulse duration $t_p = 50$ fs. However, the accuracy of this analysis suffered from the lack of appropriate procedure for simulation of the transient 2PPE signal and precise determination of $t_d = 0$.

Before discussing the TR-2PPE spectra, it is instructive to take a look at what can be learned from the transient behavior of electrons following ultrashort pulse excitation. Central issues involved in the analysis of the transient 2PPE signal in order to deduce a reliable T_1 of the IPS are:

- How to determine the lifetime T_1 of the IPS using pulses with $t_p \gg T_1$?
- How to accurately determine $t_d = 0$?
- What is the role of the total dephasing time T_2 (or pure dephasing time T_2^*) in the analysis of the spectra?
- How does the pulse duration affect the transient signal?

Some of the answers to these questions have been presented by Hertel et al. [15] in their study of electron dynamics on Cu(1 1 1) surface. By employing the OBE for a simple two-level (initial and intermediate state) model and assuming that the coherence in the final photoelectron state is immediately lost, and hence the transient population in the final state is just a replica of that in the intermediate state, they showed that a precise measurement of t_d can be made by utilizing the non-resonant 2PPE process from the SS as a reference. In this case an electron is excited from the SS into the continuum through a virtual intermediate state with a negligible lifetime and the corresponding cross-correlation trace follows directly the time profile of the pulse. Due to the finite T_1 of the IPS, on the other hand, the maximum of the IPS correlation trace appears at positive t_d after the pump pulse has passed its maximum. The solution of the OBE for the density matrix elements allows the determination of T_1 and T_2 (of the order of several to tens femtoseconds), which is much shorter than t_p. Fig. 6 shows the experimental results of the cross-correlation trace (2PPE intensity) for the SS ($n = 0$) and IPS ($n = 1$) on a Cu(1 1 1) surface with 60 fs laser pulse [15]. The maximum of the image state correlation trace is shifted by $\Delta\tau = 17$ fs with respect to the SS peak at $t_d = 0$. For the sake of data analysis the pulse width and true $t_d = 0$ were first determined from the correlation trace of the SS. The OBE of the density matrix were numerically solved to fit the measured correlation trace of the image state, from which $T_1 = 10 \pm 3$ was determined.

The OBE for a two-level ($|i\rangle$ and $|j\rangle$) system are obtained from expressions (10) and (11):

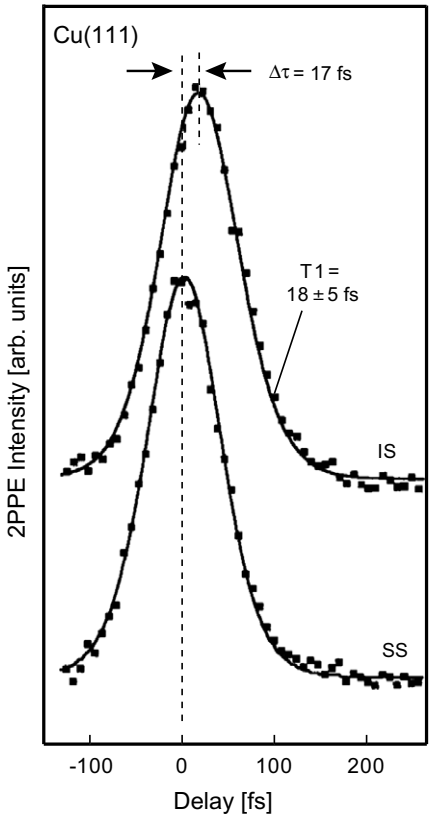

Fig. 6. Cross-correlation trace for the surface state (SS) and image potential state IS ($n = 1$) as a function of a delay t_d between pump-probe pulse (from Ref. [15]).

$$\frac{d}{dt}\rho_{jj} = -iE_{pu}(t)(\mu_{ji}\rho_{ij} - \mu_{ij}\rho_{ji}) - \frac{1}{T_1}\rho_{jj}, \tag{18}$$

$$\frac{d}{dt}\rho_{ji} = -\left[i(\epsilon_{ji} - \hbar\omega_{pu}) + \frac{1}{T_2^{ji}}\right]\rho_{ji} - i\mu_{ji}E(t)(\rho_{jj} - \rho_{ii}), \tag{19}$$

$$\rho_{ji} = \rho_{ij}^*, \quad \rho_{jj}(t) + \rho_{ii}(t) = 1, \tag{20}$$

where a closed system is assumed, i.e., the total population is conserved. For weak excitation it makes no difference if electrons are assumed to decay into empty states of the surrounding electron system [53]. Formal non-perturbative solution of (19) is given by

$$\rho_{ji}(t) = i\mu_{ji}\int_{-\infty}^{t} dt' \Delta n_{ji}(t') E_{pu}(t') e^{i[(\hbar\omega_{pu} - \epsilon_{ji}) - 1/T_2^{ji}](t-t')}. \tag{21}$$

For $t_p \gg T_2$, where the population difference $\Delta n_{ji} = \rho_{jj} - \rho_{ii}$ is assumed to remain constant over the integration interval, expression (21) can be integrated to yield

$$\rho_{ji}(t) = -i\mu_{ji}E_{\mathrm{pu}}(t)\frac{T_2^{ji}}{\mathrm{i}(\epsilon_{ji} - \hbar\omega_{\mathrm{pu}})T_2^{ji} + 1}\Delta n_{ji}(t), \tag{22}$$

and $\Delta n_{ji} = \rho_{jj} - \rho_{ii}$ satisfies the differential equation [49]

$$\dot{\Delta} n_{ji} + \left[\alpha E_{\mathrm{pu}}^2(t) + \frac{1}{T_1}\right]\Delta n_{ji} + \frac{1}{T_1} = 0, \tag{23}$$

$$\alpha = |\mu_{ji}|^2 \frac{4T_2^{ji}}{(\hbar\omega_{pu} - \epsilon_{ji})^2 T_2^{ji2} + 1}. \tag{24}$$

Under the assumption that t_{p} is much longer than all relaxation constants and for the initial condition $\Delta n_{ji}(t = 0) = -1$, this can be solved to give the excited state population

$$\rho_{jj}(t) = \frac{\alpha E_{\mathrm{pu}}^2}{\alpha E_{\mathrm{pu}}^2 + 1/T_1}\left[1 - \mathrm{e}^{-(\alpha E_{\mathrm{pu}}^2 + 1/T_1)t}\right]. \tag{25}$$

This is equivalent to the result derived from rate equations and shows a saturation at $t \gg t_{\mathrm{p}}$. In the opposite limit of $t_{\mathrm{p}} \to 0$, i.e., for the delta-function pulse $E_{\mathrm{pu}}(t) = E_{\mathrm{pu}}\delta(t)$, the excited state population shows a simple exponential decay with a time constant T_1.

For finite t_{p}, but still short compared to T_1, the excited state population starts to decay when the excitation pulse is over. In this case T_1 can be deduced from the exponentially decaying tail of the transient response at large $t \gg t_{\mathrm{p}}$. This is the case with high quantum number IPS [35] and the so-called free induction decay-sum frequency generation which measures the dephasing time T_2 of vibrational relaxation of adsorbates [41,42,44,52]. When the incident pulse varies on a time scale comparable to T_2 of the medium the rate equation approach does not apply any more and a complete set of density matrix equations must be solved.

Fig. 7 displays solutions of the OBE for the excited state population $\rho_{jj}(t)$ as a function of T_1/t_{p} at resonant excitation $\Delta\hbar\omega_{\mathrm{pu}} = 0$ by a Gaussian pulse with the duration of $t_{\mathrm{p}} = 30$ fs. Here the detuning is defined as

$$\Delta\hbar\omega_{\mathrm{pu}} = \hbar\omega_{\mathrm{pu}} - (\epsilon_j - \epsilon_i) \tag{26}$$

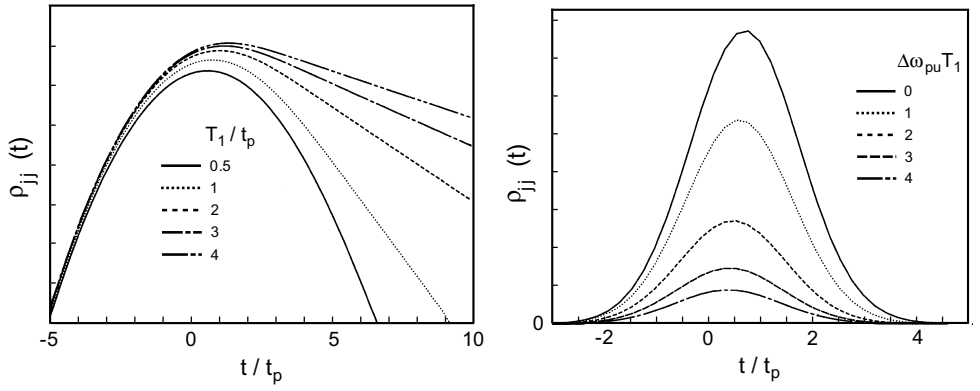

Fig. 7. Transient excited state population $\rho_{jj}(t)$ for several values of T_1/t_{p} at resonant excitation $\Delta\hbar\omega_{\mathrm{pu}} = 0$ (left panel) and for several values of $\Delta\hbar\omega_{\mathrm{pu}}T_1$ at $T_1/t_{\mathrm{p}} = 0.5$ (right panel).

and T_2^{ij} is set at 25 fs. In all cases the rising edges of $\rho_{jj}(t)$ are determined by the pulse shape. For T_1 much longer than t_p, the decay slope of $\rho_{jj}(t)$ is given by T_1, being independent of any approximation of the theoretical model or pulse shape. In this case the slope of the exponentially decaying tail at large t/t_p gives a reliable estimate of T_1. With a decrease of T_1/t_p the decay rate of $\rho_{jj}(t)$ cannot be separated from the temporal characteristics of the pulse and the maxima of $\rho_{jj}(t)$ appear at finite times (roughly proportional to T_1) shifted from $t = 0$, where the profile of the pulse is maximum. Hertel et al. [15] have shown that this shift, for which the excitation rate reaches maximum after the passage of the pump pulse maximum, provides a more reliable means to determine T_1. To this end, it is absolutely important to define the true time zero. Fig. 7 also depicts $\rho_{jj}(t)$ for different $\Delta\hbar\omega_{pu}T_1$ at $T_1/t_p = 0.5$. With increased detuning, the intensity of $\rho_{jj}(t)$ becomes weaker and the maximum of $\rho_{jj}(t)$ gradually shifts back towards $t = 0$. This is due to the fact that the larger the detuning, the faster decays the electron population in the state $|j\rangle$ caused by off-resonant excitation that is weighted by $1/(1/T_1 + |\Delta\hbar\omega_{pu}|)$ instead of T_1 at $\Delta\hbar\omega_{pu} = 0$. This is indeed the case in off-resonant 2PPE transitions from SS via virtual intermediate states with negligible T_1. In this case T_1 shorter than t_p can be determined by solving the OBE with the help of true time zero determined by the off-resonant 2PPE process from the SS as a reference.

The analysis of a two-level system is valid only if the transient 2PPE intensity can be obtained by convoluting $\rho_{jj}(t)$ with the probe pulse. This corresponds to *step-by-step* one-photon process via a real population in the intermediate state. The two-level model, however, suffers from significant shortcomings for a complete understanding of the transient 2PPE intensity given by the time integrated population in the final photoelectron states. This is due to the presence of direct two-photon ionization process involving off-resonant virtual excitation, which also produces photoelectrons with the same kinetic energy as in the *step-by-step* process.

The coupled equations for the density matrix (13) for a three-level system can be solved as a function of the pump-probe delay time t_d (see Refs. [54,55] for details) to yield the transient 2PPE spectra

$$I(\epsilon_p, t_d) = \int_{-\infty}^{\infty} \rho_{pp}(t, t_d)\mathrm{d}t. \tag{27}$$

The following set of parameters is used for the Gaussian pump and probe pulses: $\hbar\omega_{pr} = 2.5$ eV and $t_{pu} = t_{pr} = t_p = 30$ fs. The time constants are taken as $T_1 = 50$ fs, $T_2^{ji/pi/pj} = 25$ fs. Here the zero of energy is the vacuum level, $\epsilon_i = -6.0$ eV and $\epsilon_j = -1.0$ eV. The calculated 2PPE spectra are shown in Fig. 8 as a function of photoelectron kinetic energy for different time delays $t_d = 0$, 30 and 70 fs at $\Delta\hbar\omega_{pu} = 0.1$ eV. For $t_d = 0$ there appear two overlapping peaks as indicated. One is due to the process (a) in Fig. 1 via the intermediate state of ρ_{jj}, whose signal survives for a period determined by T_1. The other peak is due to excitation from the initial state denoted as the process (b) in Fig. 1. The peak intensity due to (a) increases up to approximately $t_d \simeq T_1$ and then decreases with further increase of t_d. It is important to remark that at small t_d the 2PPE intensity observed at the photoelectron kinetic energy corresponding to the intermediate state peak contains a contribution from the tail of the direct process from the initial state peak. This is the region in which a simple two-level model cannot be applied to the analysis of transient 2PPE response. Fig. 8 also reveals that the linewidth of the intermediate state peak depends on t_d, i.e., it is larger when the pump and probe pulses overlap in

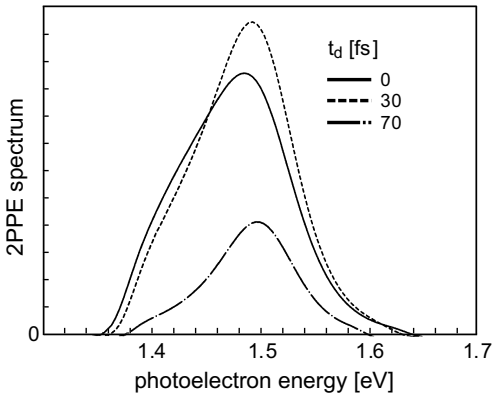

Fig. 8. TR-2PPE spectra as a function of t_d between the pump and probe pulses of duration $t_p = 30$ fs. The detuning is set at $\Delta_{pu} = 0.1$ eV.

time (compare the widths corresponding to $t_d = 0$ and $t_d = 30$ fs with that of $t_d = 70$ fs). This spectral narrowing as a function of t_d has been observed on Cu(1 1 1) [18] and on Ag(1 0 0) [50]. The present analysis supports the explanation given by Shumay et al. [34] who attributed the linewidth narrowing to the interplay between the *step-by-step* one-photon process and the direct two-photon ionization. The latter process is effective only in the presence of the overlapping pump and probe pulses. The temporal population in the intermediate state due to non-resonant process occurs during this time interval. At longer t_d when the probe pulse is decoupled from the pump pulse, only the *step-by-step* process remains responsible for the appearance of the intermediate state peak, thereby carrying information on the transient decay of the intermediate state population.

The t_d dependence of TR-2PPE spectra was theoretically studied in detail using OBE for a three-level system and applied to the IP states on a Cu(0 0 1) surface [56,57]. It was demonstrated that if the pulse durations are comparable to or shorter than T_1 of the intermediate states, the linewidth measured in an energy-resolved 2PPE spectrum depends on t_d, i.e., it continues to decrease in going from negative t_d to positive t_d, and crucially depends on the shape of the pump and probe pulses. Similar behavior has been obtained for time-resolved vibrational sum-frequency generation spectra from adsorbates [58].

As the detuning increases by going away from resonant excitation, the initial state peak shifts to lower energy side with a rapid decrease in the intensity, and eventually disappears in the absence of the overlap between the pump and probe pulses. However a portion of the *step-by-step* component included in the direct process remains near the intermediate state peak, which may influence the cross-correlation trace measured in the vicinity of the resonance. Although at off-resonant excitation the linewidth of the 2PPE spectrum observed by using continuous fields, or pulses sufficiently longer than T_1, is given by T_2^{ij}, it is found that an ultrashort pulse duration, comparable with the phase relaxation time of the medium, produces a tail in the 2PPE spectrum as a consequence of the overlap of pump and probe pulses.

Fig. 9 shows the transient 2PPE response (27) at photelecton energy tuned to the intermediate state peak for several values of $\Delta\hbar\omega_{pu}T_1$. The maxima shift from $t_d = 0$ in a similar manner as the transient population $\rho_{jj}(t)$ in the intermediate state. It should be noted

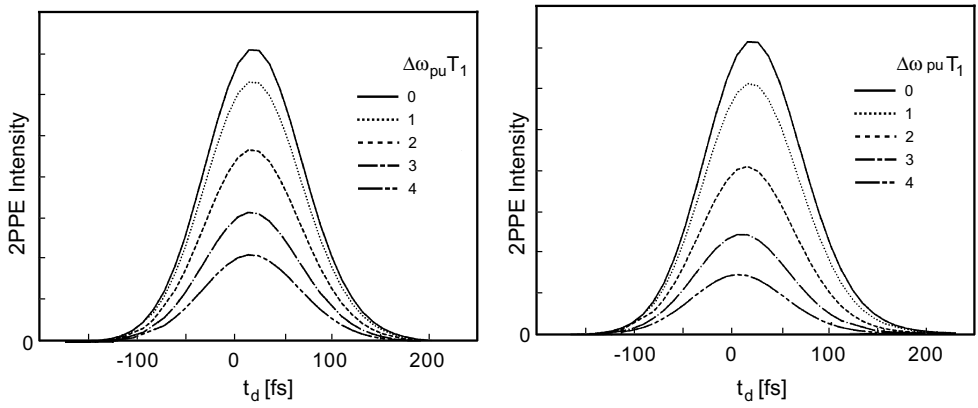

Fig. 9. Transient response of intermediate state for various detuning $\Delta\hbar\omega_{pu}T_1$ at the kinetic energy of photoelectrons tuned to the intermediate state peak (left panel). The kinetic energy of photoelectrons is tuned to the initial state peak (right panel).

that this similarity between $\rho_{jj}(t)$ and the transient 2PPE response is expected only when the pump and probe pulse durations are shorter than T_1. Otherwise the transient response of photoelectrons is determined by the longer (pump or probe) pulse. The intensity continues to decrease with increasing $\Delta\hbar\omega_{pu}T_1$ because of the decreasing transition probability of photo-excitation by the pump pulse. It is needless to mention that when the pulse duration is much longer than T_1, there appears no shift of the maximum from $t_d = 0$. In the case where $T_1 > t_p$ and t_d is large, the intensity exhibits an exponential decay with the time constant T_1. This is the region where the decay rate is independent of the exact pulse shape or duration and is simply the lifetime of the intermediate state. Accordingly, if the lifetime is longer than the pulse duration, it can be reliably deduced from the exponentially decaying tail of the transient 2PPE signal, as has been observed for the higher IP states on Cu(100) and Ag(100) [34].

Fig. 9 also shows the transient 2PPE intensity tuned to the initial state peak. With increasing $\Delta\hbar\omega_{pu}T_1$ the position of the maximum shifts towards $t_d = 0$. This is due to the fact that in the process (b) the photo-excited electrons cannot populate the intermediate state in a real process and electrons are brought above the vacuum level during a narrow temporal period of the overlap of the pump and probe pulses. However, at larger t_d and small $\Delta\hbar\omega_{pu}$ the process (a) becomes dominant over the process (b) because of a finite T_1 involved in the former process.

As we have demonstrated in the above analyses, the existence of two different channels (a) and (b) that produce the intermediate state peak in TR-2PPE spectra requires the cross-correlation trace to be observed under non-resonant condition free from the influence due to the direct two-photon process. Even so one should be aware that the direct two-photon process also contributes to the cross-correlation trace near $t_d = 0$ and at small detuning from the resonance. It is also important to mention the influence of the pulse shape. In the present numerical analysis the Gaussian-shape for the pulse envelope was used, which decays faster than the exponential decay of the electronic system. This allows us to distinguish which tails govern the decaying feature of the 2PPE signal. The decay of the overlap between pump and probe pulses as a function of t_d plays an important role in the peak shift of the cross-correlation trace near $t_d = 0$ or the excited state population near

$t_d = 0$ for t_p longer than T_1. Only when this overlap decays exponentially near $t_d = 0$, detuning influences the estimate of T_1 from the transient 2PPE signal. When t_p is much shorter than T_1 and T_2 the shape of the pulse envelope has no influence on the transient 2PPE signal.

4. Microscopic descriptions of dephasing and decay of initial and intermediate states in 2PPE

Despite the fact that already the earliest microscopic theories of photoemission induced by two photon absorption in atoms [9] and at solid surfaces [5,11] had been formulated within microscopic, strictly quantum-mechanical framework, the obtained expressions for the photoabsorption rate and/or photoemission yield have not been extensively used in the analyses and interpretations of 2PPE experiments. Rather, the results of the majority of experiments have been interpreted by resorting to simpler phenomenological approaches based on the OBE described and discussed in the preceding sections. In this section we shall first attempt to identify the difficulties connected with the practical application of microscopic theories that have lead to this situation, and then discuss recent theoretical progress that may enable a full implementation of the microscopic approach in the future analyses of 2PPE spectra.

Quite generally, theoretical expressions for the two-photon absorption (2PA) rates and 2PPE yield and spectra are given in terms of the dipolar matrix elements for the interaction of the photon field with the electronic structure of the system, on the one hand, and the quasiparticle propagators describing the motion of photo-excited electrons and holes during the various stages of 2PA and 2PPE [5,9,11,13,14], on the other hand. In real systems the motion of excited quasiparticles is affected by static interactions with the various defects and dynamic interactions with other electrons and excitations constituting the heatbath of the system. Scattering by defects gives rise to incoherent phase changes whereas interactions with the dynamic degrees of freedom give rise to both the decay and phase changes in the wavefunctions of excited quasiparticles. This implies that the corresponding propagators and mutual interactions should be calculated by taking into account these effects, analogously to the procedures employed in the many-body theory of one-photon-photoabsorption [59] and photoemission [8].

The calculation of dipolar matrix elements describing interactions of the pump and probe photon fields with surfaces requires the knowledge of the electronic structure of the studied systems and this type of information is becoming available only recently. Equally important is a proper treatment of the various interactions that affect propagation of quasiparticles during the various stages of two-photon photo-excitation process by laser pulses of finite duration. The absence of reliable information on these basic components of the 2PPE expressions has hindered their application in the analyses of experimental data. In this situation the phenomenological approaches based on the OBE pertaining to restricted two- or three-level models (see preceding sections) could provide faster intuitive and semiquantitative descriptions of the 2PPE spectra. Neglecting the energy dependence of the dipolar matrix elements in the few level models, which would otherwise arise from the band structure of the studied systems, it turned out possible, and in many circumstances satisfactory, to model or fit the characteristics of the 2PPE spectra from surface bands by three relaxation times $1/\Gamma^*$, T_1 and T_2^*, as outlined in the preceding section. However, such procedures have left the microscopic, physical origin of these phenomenological parameters largely unexplained.

Noticable progress in providing microscopic descriptions of quasiparticle propagation in surface bands has been made in the past decade by the San Sebastian group and their collaborators[60]. Adopting the pseudopotential description for one-electron states in metal bands they have carried out a series of calculations of asymptotic lifetimes (decay rates) of quasiparticles in the surface and image potential bands by resorting to the Fermi golden rule (FGR) approach or its improvements like the GW-approximation (GWA) [60]. The description of the asymptotic quasiparticle decay expressed in terms of the thus obtained lifetimes is valid on the time scales of few tens of femtoseconds and longer. This enables the construction of asymptotic forms of the corresponding quasiparticle propagators in the time domain [13] as well as in the energy domain [11].

The application of the FGR approach and its improvements in descriptions of decay and decoherence of quasiparticles is based on the assumption of adiabatic switching on of the quasiparticle interactions with the excitations of the heatbath of the system. However, in the first step of 2PPE from surface bands the elementary process of pump photon absorption suddenly creates an intermediate coherent electron–hole pair whose subsequent propagation and (de)coherence is then probed by the second (probe) photon beam. This means that the interactions of two photo-excited quasiparticles (electron and hole) with the excitations of the heatbath and among themselves are switched on non-adiabatically [61], in contrast to what is assumed in the FGR and related calculations of the quasiparticle decay rates. Since the adiabatic descriptions do not account for the transient effects in relaxation processes they miss out some of the important effects that may manifest themselves in the spectra recorded on the ultrashort time scale [62].

Let us consider a prototype example of the first step of 2PPE in which absorption of a pump pulse photon excites an electron from a state in the occupied part of a two-dimensional (2D) surface band (Shockley state) into an unoccupied state within one of the image potential bands. This process may be viewed as a creation of a coherent intermediate electron–hole pair or a dynamical dipole over the initial equilibrium state of the system. Since the momentum of the absorbed photon is negligible, the initial momenta of photo-excited electron and hole (in this case their initial quantum numbers) are of equal magnitude and opposite sign. The two quasiparticles are entangled in the many-body wave function of the system in the sense that a measurement of the momentum of one of them would also reveal the momentum of the other. Then, in the absence of changes of the *effective* interactions of excited quasiparticles with the environment during optical transitions, the excited IPS-SS electron–hole pair would continue to propagate without loosing its initial coherence. However, optical excitation of an e–h pair in the system destroys its initial equilibrium which results in switching on of the effective interactions of two excited quasiparticles with each other, with the fluctuations in the system represented by its dynamical degrees of freedom, and with the various scattering centers. These interactions will give rise to decoherence of the initially coherent electron–hole pair in the course of time. Here we shall focus our attention on the interactions with dynamical degrees of freedom which cause real and virtual intra and interband transitions of quasiparticles. In the terminology of OBE discussed in the preceding sections these processes give rise to the density (energy) and phase relaxation of the states partaking in 2PPE from surface bands.

Among the quasiparticle interactions with the various degrees of freedom constituting the system heatbath (electronic, magnetic, vibrational excitations, etc), we shall in the following consider only the coupling to the electronic charge density fluctuations (single and multipair excitations and collective modes) whose dynamics can be adequately described

by the charge density response functions. In this case the screened Coulomb interactions of quasiparticles with the heatbath and between themselves can be represented by equivalent interactions with a boson field whose spectrum of excitations is equal to the spectrum characteristic of the electronic response of the system [65,66]. The rationale of this equivalent boson approach is easy visualization of the various interactions and processes that can give rise to decoherence of electron–hole pairs in the intermediate states of 2PPE.

Fig. 10 illustrates several elementary excitation processes subsequent to pump photon absorption in 2PPE from surface bands in which virtual and real quanta of bosonized excitations of the system heatbath are exchanged (a) between a single IPS-electron and the metal, (b) between a single SS-hole and the metal, and (c) between the IPS-electron and SS-hole. The processes (a) and (b) give rise to the heatbath induced decay and dephasing of single quasiparticles that form the excited IPS-SS electron–hole pair in the intermediate state of 2PPE. On the other hand, the process (c) gives rise to the heatbath mediated decay and dephasing of the intermediate electron–hole pair (cf. Ref. [62]). Note, however, that all three processes (a), (b) and (c) contribute to the decay and dephasing of the photo-excited e–h pair as a whole. The quantum mechanical probability amplitudes of these processes can be formulated for quasiparticle interactions with each particular type of excitations of the heatbath. The corresponding probabilities expressed as functions of the propagation time provide information on the characteristics and importance of each decoherence mechanism that affects propagation of IPS-SS electron–hole pairs in the intermediate

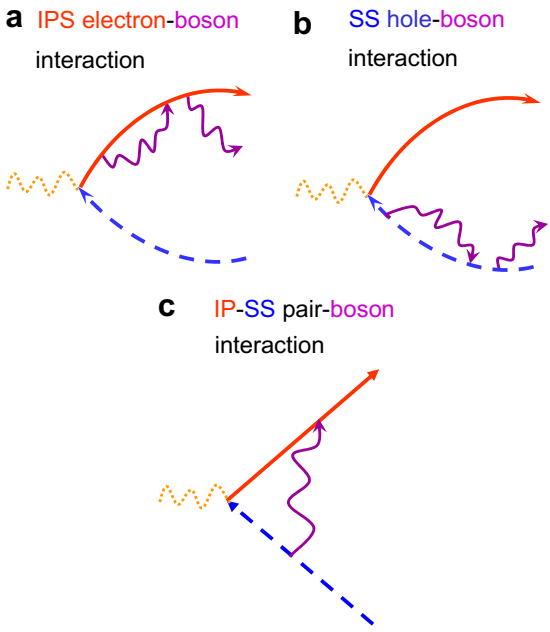

Fig. 10. Elementary interactions of quasiparticles in the intermediate states of 2PPE with bosonized excitations constituting the system heatbath. Wiggly dotted line denotes the pump photon which excites an IPS-SS electron–hole pair, full and dashed lines denote electron and hole propagators, respectively, and full wiggly lines denote propagators of bosonized excitations constituting the system heatbath. (a) Processes in which an IPS-electron exchanges one virtual and one real boson excitation with the system heatbath. (b) Same for a SS-hole. (c) Lowest order process in which an IPS-electron and SS-hole exchange one excitation quantum of the system heatbath.

states of a 2PPE event. In the following we shall discuss the situation in which the excited IPS-electrons and SS-holes couple to the heatbath of electronic excitations in the system.

Fig. 11 shows the total transition probabilities $P_{\mathbf{K},n}(t)$ pertaining to the processes in which an IPS-electron or a SS-hole, created in the respective bands on Cu(1 1 1) surface with initial parallel-to-the-surface wavevector $\mathbf{K} = 0$, can make only intraband transitions to other states $|\mathbf{K}'\rangle \neq |\mathbf{K}\rangle$ by exciting n real excitation quanta of the electronic charge density fluctuations in the system, whose lowest order contributions are depicted in Figs. 10a and b. A specificity of the present example is that an electron created at (injected to) the bottom of an empty IPS-band cannot dissipate energy and momentum through real intraband energy- and momentum-conserving transitions. Hence, the corresponding transition probabilities saturate for long times at a finite value (<1) which keeps track of the initial off-the-energy-shell transient excitation of the heatbath quanta that can take place within the Heisenberg uncertainity window. In contrast to this situation, a hole created at the bottom of the SS-band can decay towards the Fermi level through real excitations of the heatbath quanta. This results in a rather complex early behaviour of $P^{(SS)}_{\mathbf{K}=0,n=1}$ that tends first to a linear t-dependence after the initial transient dies out. For long times it saturates at a constant value <1 in accord with the unitarity requirement (cf. Fig. 1 in Ref. [62]). Both results demonstrate a non-Markovian early evolution of the quasiparticles. This behaviour should be compared with the FGR result displayed for the same process in asymptotic Markovian description of the SS-hole evolution, which remains strictly linear in t throughout the evolution interval. Additionally shown in Fig. 11 is the probability for two-boson ($n = 2$) excitations induced by intraband transitions of the SS-hole, and in the same evolution interval this quantity is noticeably smaller than the one-boson excitation probability.

Fig. 12 shows temporal dependence of the probability of heatbath mediated decoherence $P^{(offd)}_{\mathbf{K}=0,n=0}$ for an initially coherent electron–hole pair excited in the IPS- and SS-bands on a Cu(1 1 1) surface for the initial quasiparticle states at the bottom ($\mathbf{K} = 0$) of the

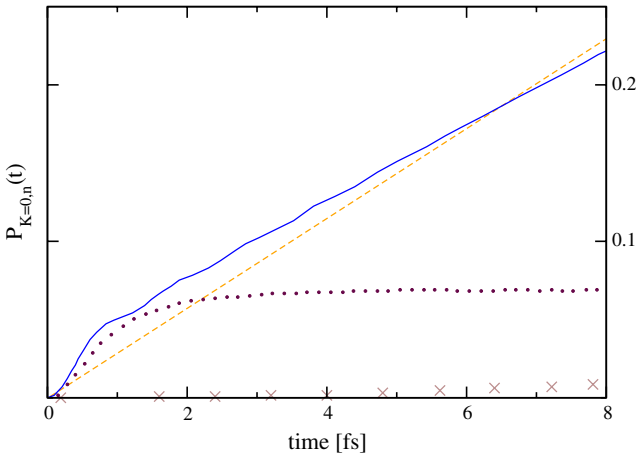

Fig. 11. Single particle intraband transition probabilities into a final state involving one electronic excitation quantum for SS-hole, $P^{(SS)}_{\mathbf{K}=0,n=1}$ (full line), and IPS-electron $P^{(IP)}_{\mathbf{K}=0,n=1}$ (doted line), on Cu(1 1 1) surface. Dashed line denotes the SS-hole Fermi golden rule (FGR) intraband transition probability $\propto t$. Crosses denote the SS-hole intraband transition probability $P^{(SS)}_{\mathbf{K}=0,n=2}$ involving emission of two bosonized electronic excitation quanta.

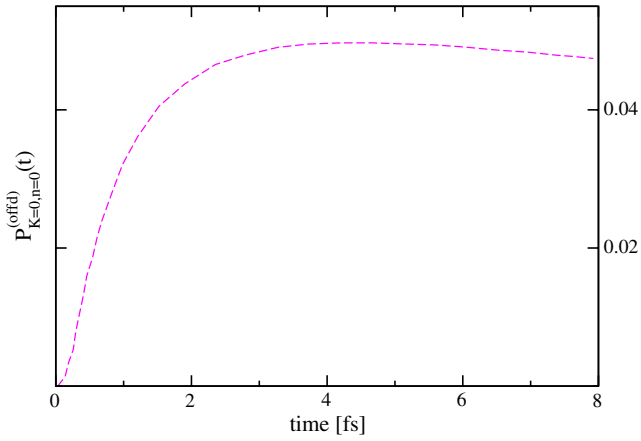

Fig. 12. Probability of heatbath mediated decoherence process $P^{(\mathrm{offd})}_{\mathbf{K}=0,n=0}$ corresponding to the diagram in Fig. 10c in which the exchange of bosonized substrate excitations induces intraband transitions of the quasiparticles constituting the IPS-SS electron–hole pair.

respective bands (process corresponding to the diagram depicted in Fig. 10c). After a steep rise up to a maximum that is reached in the first few femtoseconds, the probability $P^{(\mathrm{offd})}_{\mathbf{K}=0,n=0}$ slowly falls off and asymptotically saturates at a finite value. In this process each quasiparticle undergoes an off-diagonal transition (hence superscript offd) but the total number of excited bosons in the final state of the system remains zero (hence subscript $n = 0$), since only the boson emission followed by reabsorption process takes place. Comparison of Figs. 11 and 12 reveals much larger effects on the quasiparticle decay coming from the processes shown schematically in Fig. 10a and b than of the effects from the processes depicted in Fig. 10c.

Examples of the inelastic transitions probabilities involving exchange of excitation quanta between the system heatbath and optically excited electron–hole pairs in IPS- and SS-bands on Cu(1 1 1) shown in Figs. 11 and 12 clearly demonstrate that the early evolution of quasiparticles in the intermediate states of 2PPE from surface bands strongly deviate from the Markovian behaviour. Due to this their propagation on the ultrashort time scale cannot be described in terms of the asymptotic rate constants deriving from the FGR or its improvements like the GWA. Hence, the treatment of evolution of intermediate states of 2PPE that would go beyond the asymptotic descriptions based on the rate constants are needed for getting a better insight into the ultrafast dynamics governing the TR-2PPE spectra.

The first systematic studies of the effects of the various electronic interactions that influence the TR-2PPE spectra from surface bands in the preasymptotic regime (i.e., for finite observation/detection time of electrons populating the final states of 2PPE) were undertaken by Sakaue et al. [63,64]. These authors have developed a theory of TR-2PPE processes based on the Keldysh non-equilibrium Green's function formalism by taking into account both the direct and indirect populations of the intermediate states, the effects of Coulomb interaction between photo-excited electron–hole pairs, as well as the influence of relaxation of secondary electrons and holes (equivalent to selfenergy corrections in phenomenological parametrization of the 2PPE spectra). When an IPS is populated from a SS, and not from the bulk continuum, the electron trapped in front of the metal surface

experiences an additional potential arising from the presence of a hole localized at the surface. This excitonic type of interaction which may influence the relaxation dynamics of the intermediate state was discussed above in the context of heatbath mediated e–h interactions (cf. Fig. 10c). The solution of the problem of 2PPE for finite observation times was sought within a perturbational approach using parametrized interactions and the forms of single particle propagators that, for the sake of simplicity, were phenomenologically renormalized through the FGR decay rates that lead to the asymptotic decay of quasiparticle states analogous to the ones appearing in the applications of the OBE. Unfortunately, this restricts the validity of the descriptions of various microscopic processes to the same domain of validity as of the asymptotic representations of quasiparticle propagators (i.e., to the regime of few tens of femtoseconds and longer). The thus formulated approach was used to analyse the differences between the 2PPE spectra calculated from the non-equilibrium Green's functions many-body approach and the OBE for different sets of model parameters and decay rates. Several interesting results have emerged from these analyses, the most important ones being: (i) the absence of the need for introducing the "pure dephasing" times in the many-body approach since such effects are correctly contained in the quantum mechanical formulation of the latter formalism, and (ii) even for negligible effective interactions between IPS electron and SS-hole (represented by the heatbath mediated or excitonic-like interactions shown in Fig. 10c), the populations of final 2PPE electron states and yield strongly depend on the decay of *both* the intermediate electron and hole states [64]. Therefore, a proper quantum description of 2PPE experiments require the knowledge of both the electron and hole intermediate state propagators.

An imminent conclusion resulting from the above discussions is that future advances in the development of microscopic descriptions of TR 2PPE that would be valid in the true femtosecond domain necessitate appropriate non-asymptotic approach to ultrafast quasiparticle dynamics in surface bands [62,65]. This information is contained in the temporal dependence of the corresponding quasiparticle propagators in the real time domain. Recent progress in this direction has been made by Lazić et al. [66] who have developed a many-body description of non-adiabatic dynamics of electrons and holes in surface bands valid on the extreme ultrashort time scale by combining the selfconsistent treatment of electronic response of metal surfaces [67] with the formalism for calculation of survival probabilities of electrons and holes created in the unoccupied and occupied $|\mathbf{K}\rangle$-states of surface bands [65], respectively. In this approach the quasiparticle survival probability $L_{\mathbf{K}}(t)$ in a particular band is calculated from the absolute square of the corresponding *single particle* Green's function $G_{\mathbf{K}}(t)$ expressed in cumulant representation [65,66]:

$$L_{\mathbf{K}}(t) = |G_{\mathbf{K}}(t)|^2 = |\exp[C(\mathbf{K},t)]|^2, \tag{28}$$

where $C(\mathbf{K},t)$ is the sum of all cumulants generated by the interaction of the quasiparticle with bosonized excitations of the system heatbath. In the present problem the dominant contribution comes from the second order cumulant $C_2(\mathbf{K},t)$ which can be calculated exactly [65] once the surface electronic structure and the charge density response function of the system is known [67].

Fig. 13 shows the survival probabilities for an electron and a hole injected into a momentum eigenstate $|\mathbf{K}\rangle$ of energy $\epsilon_{\mathbf{K}}$ in the IPS- or SS-band on the Cu(1 1 1) surface, in the time interval $0 < t < 10$ fs. In the ultrashort early interval set by the Heisenberg uncertainity the evolution of $C_2(\mathbf{K},t)$ follows the universal "Zeno behaviour"

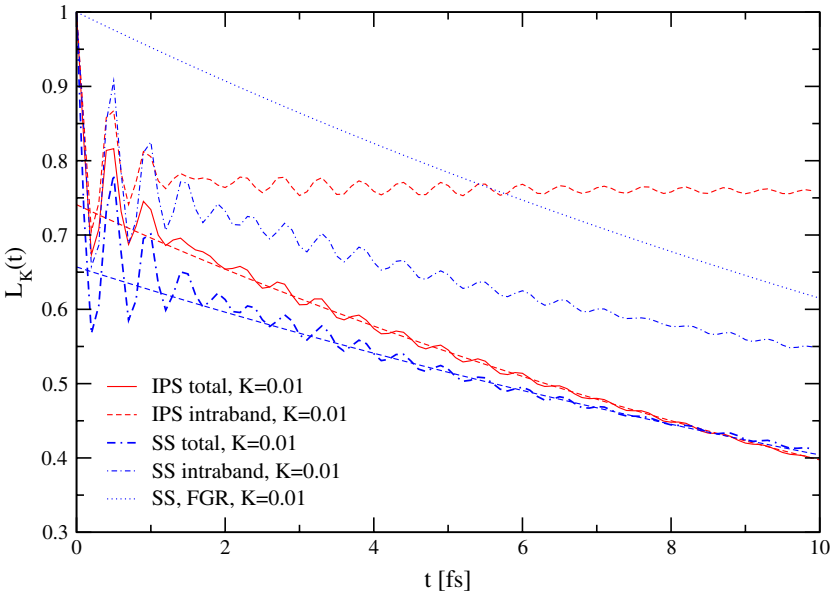

Fig. 13. Total survival probability $L_{\mathbf{K}}(t)$ for an electron and hole promoted into the surface state band and the first image potential band on Cu(1 1 1) surface, respectively, with the initial state wavevector $K = 0.01$ a.u. (see legend for assignments). Asymptotic decay produced by the "corrected" FGR law (Eq. (30)) is shown by dashed curves and the "bare" FGR exponential decay of the SS-hole by dotted curve. The survival probabilities calculated in the presence of intraband transitions only are also shown for comparison (upper dashed and dash-dotted curves for IPS-electron and SS-hole, respectively).

$$C_2(\mathbf{K}, t \to 0) = -t^2/2\tau_Z^2 + \mathcal{O}(t^3), \tag{29}$$

where τ_Z is the so-called Zeno time [68]. Hence, the initial drop of the survival probability (28) follows a Gaussian law reflecting the quasiballistic initial propagation of both types of quasiparticles. This behaviour is superseded by a superposition of oscillations arising from the non-adiabatic (off-resonant) excitations of surface plasmons in the metal and a gradual build up of the population decay arising from the resonant excitation of e–h pairs in the metal. Due to the off-resonant character of plasmon excitations their amplitude diminishes in the course of time. All these features signify a non-Markovian dynamics in the early evolution of quasiparticles. As t increases the amplitudes of on-the-energy-shell scattering processes become dominant and in this regime the cumulant exponent in (28) can be well approximated by the "corrected" FGR law:

$$C_2(\mathbf{K}, t > \Gamma_{\mathbf{K}}^{-1}) \to -(\Gamma_{\mathbf{K}}/2 + i\Lambda_{\mathbf{K}})t - w_{\mathbf{K}}, \tag{30}$$

which gives rise to a renormalized exponential decay of the quasiparticle survival probability. Here $\Gamma_{\mathbf{K}}$ is the FGR decay rate of a quasiparticle with the initial momentum $\mathbf{K}$ in the surface band (i.e., IPS or SS). $\Lambda_{\mathbf{K}}$ is a shift of the energy level $\epsilon_{\mathbf{K}}$ in the respective band which arises from polarization of the heatbath by the interaction with the excited quasiparticle. The time independent term $w_{\mathbf{K}}$ is off-resonant correction to the first two terms on the RHS of (30) and measures the non-adiabaticity of relaxation processes following

the non-adiabatic switching on of the quasiparticle interaction with the excitations of the heatbath.

As expected, the preasymptotic survival probabilities shown in Fig. 13 exhibit a non-Markovian behaviour before the formation of a steady $w_{\mathbf{K}}$-corrected FGR decay (30) for $t > 10$ fs. The survival probabilities obtained from the corrected FGR decay (30) are also plotted for comparison and it is seen that during the first few femtoseconds they strongly deviate from the exact preasymptotic behaviour. It is also noteworthy that the bare FGR decay $\exp(-\Gamma_{\mathbf{K}}t)$ gives a poor description of the quasiparticle propagation in the preasymptotic evolution interval, as exemplified in Fig. 13 for a hole created at the bottom of the SS-band.

The contributions to the second order cumulant $C_2(\mathbf{K}, t)$ that governs the decay of the survival probability may arise both from intraband and interband transitions of the quasiparticle. To illustrate this feature we also show in Fig. 13 the IPS-electron and SS-hole survival probabilities calculated in the presence of intraband transitions only. Here we find that the contribution from intraband IPS $\rightarrow$ IPS electron transitions to the resonant decay rate $\Gamma_{\mathbf{K},\mathrm{IPS}}$ is insignificant for $K = |\mathbf{K}| = 0.01$ a.u. as only very small initial kinetic energy is available for excitation of other electrons in the system. On the other hand, their role is dominant in the off-resonant excitation of surface plasmons and a gradual build up of the non-adiabatic correction $w_{\mathbf{K},\mathrm{IS}}$. Thus, the non-vanishing decay rate $\Gamma_{\mathbf{K},\mathrm{IPS}}$ at this small value of K is almost solely due to IPS-electron interband transitions into the SS ($\sim$39%) and bulk bands ($\sim$61%).

In contrast to the case of IPS-electron, for a SS-hole with initial $K = 0.01$ a.u. the intraband SS $\rightarrow$ SS transitions contribute the major part ($\sim$70%) to the total decay rate $\Gamma_{\mathbf{K},\mathrm{SS}}$. They also give dominant contribution ($\sim$60%) to the short time behavior of the survival probability which is reflected in the value of the total non-adiabatic correction $w_{\mathbf{K},\mathrm{SS}}$ that considerably reduces the magnitude of $L_{\mathbf{K}}(t)$.

We may summarize the results obtained for the quasiparticle survival probabilities shown in Fig. 13 by observing that they enable the identification of three distinct regimes of ultrafast quasiparticle dynamics in IPS- and SS-bands on Cu(1 1 1). The early Gaussian decay regime ($0 < t < 1$ fs) is followed by preasymptotic non-Markovian evolution with superimposed off-resonant excitation of surface plasmons and resonant excitation of e–h pairs in the metal. This structure persists up to $t \sim 10$ fs and only past that time the off-resonant plasmon excitations die out and the steady state asymptotic evolution governed by the *corrected* FGR decay (30) takes over. However, even long past that time the bare FGR decay of the quasiparticle survival probability, $\exp(-\Gamma_{\mathbf{K}}t)$, is not yet approached, signifying that extreme ultrafast dynamics of quasiparticles promoted in surface bands requires preasymptotic description of relaxation and decay processes. Hence, further progress in theoretical interpretations of the 2PPE spectra should be sought in terms of the above elucidated quasiparticle evolution and the corresponding propagators rather than their approximations based on the asymptotic rate constants.

5. Conclusion

In this review we have discussed several quantum-mechanical approaches employed in the analyses of the spectral features of photoelectron yield in 2PPE from electronic states localized at metal surfaces. Special attention has been focused on the application of optical Bloch equations (OBE) in the discussion of relaxation dynamics of electrons excited in

image potential states (IPS) that play the role of intermediate states in 2PPE. One of the most noticeable findings in modeling the energy-, and time-resolved 2PPE spectra of IPS by OBE pertains to the need of invoking pure electronic dephasing between the ground and the excited states, otherwise no spectral intensity can be retrieved from the initially unoccupied IPS. Relaxation times T_1 and T_2 invoked to describe the dynamics of intermediate states can be determined by combining the intrinsic linewidth measurements in high-resolution energy-resolved 2PPE with the analyses of cross-correlations obtained from TR-2PPE experiments. Both types of 2PPE measurements should be performed at off-resonant excitation in order to avoid the influence of direct two-photon ionization from the initial state.

It has been concluded that T_1 can be directly obtained from the slope of logarithmic plot of the transient response at sufficiently large t_d for $T_1 \gg t_p$. In the opposite limit of $T_1 \ll t_p$, the exponential temporal decay of the transient response cannot be separated from the pump-probe cross-correlation and numerical fitting of the solution of the OBE for the transient 2PPE signal observed at non-resonant excitation is required. Although temporal resolution can be improved by using shorter pulses at the expense of energy resolution, the contribution of non-resonant processes increases because of the more relaxed energy conservation requirement. However, these arguments can not be applied to adsorbates on metal surfaces. Thus, for example, in the case of $2\pi^*$ level of CO molecules on Cu(1 1 1), the energy-, and time-resolved 2PPE studies could only indicate a lower limit of about 1 fs for T_2 [24] and an upper limit of $T_1 = 5$ fs [23]. For such an exceptionally short-lived excited state with a lifetime of the order of or below a femtosecond, the correlation trace is dominantly governed by the pulse characteristics and transient effects so that it is difficult to make unambiguous estimates of T_1.

As the laser pulse duration becomes shorter and shorter, the resonance and off-resonance conditions lose their meaning because of the Heisenberg uncertainty principle. In this regime the dephasing processes cannot be described in terms of asymptotic rate constants and the studies of ultrafast electron dynamics require a non-Markovian treatment going beyond the solutions of phenomenologically parametrized OBE given by expressions (10) and (11). First attempts in this direction, together with the indications of further progress in applying the microscopic theories to interpret the 2PPE spectra from surface bands were outlined in Section 4.

Acknowledgements

The first author (H.U.) would like to thank Profs. M. Wolf and U. Höfer for stimulating discussions, and Dr. T. Mii for discussions and help in numerical calculations. The second author (B.G.) would like to acknowledge the hospitality extended to him during a short term visit to the University of Toyama. The work in Zagreb was supported by the Ministry of Science, Education and Sports of Republic of Croatia through the Research Contract No. 035-0352828-2839.

References

[1] J.B. Pendry, in: B. Feuerbacher, B. Fitton, R.F. Willis (Eds.), Photoemission and the Electronic Properties of Surfaces, Wiley, Chichester, 1978.
[2] E.W. Plummer, W. Eberhardt, Adv. Chem. Phys. 49 (1982) 533.

[3] E.W. Plummer, C.T. Shen, W.K. Ford, W. Eberhardt, R.P. Messmer, H.-J. Freund, Surf. Sci. 158 (1985) 58.
[4] R. Haight, Surf. Sci. Rep. 21 (1995) 275.
[5] I. Adawi, Phys. Rev. 134 (1964) A788.
[6] G.D. Mahan, Phys. Rev. B 2 (1970) 4334.
[7] W. Schaich, N.W. Ashcroft, Phys. Rev. B 3 (1971) 2452.
[8] C. Caroli, D. Lederer-Rozenblatt, B. Roulet, D. Saint-James, Phys. Rev. B 8 (1973) 4552.
[9] M. Göppert-Mayer, Ann. Phys. 9 (1931) 273.
[10] T. Fauster, W. Steinmann, in: P. Halevi (Ed.), Electromagnetic Waves: Recent Development of Research, Photonic Probes of Surfaces, Elsevier, Amsterdam, 1995, pp. 347–411.
[11] H. Ueba, Surf. Sci. 334 (1995) L719.
[12] H. Petek, S. Ogawa, Prog. Surf. Sci. 56 (1997) 239.
[13] C. Timm, K.H. Bennemann, J. Phys.: Condens. Matter 16 (2004) 661.
[14] M. Sakaue, J. Phys.: Condens. Matter 17 (2005) S245.
[15] T. Hertel, E. Knoesel, M. Wolf, G. Ertl, Phys. Rev. Lett. 76 (1996) 535.
[16] S. Pawlik, R. Burgermeister, M. Bauer, M. Aeschlimann, Surf. Sci. 402–404 (1998) 556.
[17] D. Velic, E. Knoesel, M. Wolf, Surf. Sci. 424 (1999) 1.
[18] T. Hertel, E. Knoesel, A. Hotzel, M. Wolf, G. Ertl, J. Vac. Sci. Technol. A 15 (1997) 1503.
[19] M. Wolf, A. Hotzel, E. Knoesel, D. Velic, Phys. Rev. B 59 (1999) 5926.
[20] B. Gumhalter, K. Wandelt, Ph. Avouris, Phys. Rev. B 37 (1988) 8048.
[21] H. Ueba, in Ref. [10], pp. 211–305.
[22] See, for example H.-L. Dai, W. Ho (Eds.), Laser Spectroscopy and Photo-Chemistry on Metal Surfaces, World Scientific, Singapore, 1995.
[23] L.B. Bartels, G. Meyer, H. Rieder, D. Velic, E. Knoesel, A. Hotzel, M. Wolf, G. Ertl, Phys. Rev. Lett. 80 (1998) 2004.
[24] E. Knoesel, T. Hertel, M. Wolf, G. Ertl, Chem. Phys. Lett. 240 (1995) 409.
[25] J.W. Gadzuk, Chem. Phys. 251 (2000) 87.
[26] J.A. Prybyla, H.W.K. Tom, G.D. Aumiller, Phys. Rev. Lett. 68 (1992) 503.
[27] W. Steinmann, Appl. Phys. A 49 (1989) 365.
[28] W.R. Merry, R.E. Jordan, D.P. Padowitz, C.B. Harris, Surf. Sci. 295 (1993) 393.
[29] W. Wallauer, Th. Fauster, Surf. Sci. 374 (1997) 44.
[30] S. Schuppler, N. Fischer, W. Steinmann, R. Schneider, E. Bertel, Phys. Rev. B 42 (1990) 9403.
[31] S. Schuppler, N. Fischer, Th. Fauster, W. Steinmann, Phys. Rev. B 46 (1992) 13539.
[32] M. Wolf, E. Knoesel, T. Hertel, Phys. Rev. B 54 (1996) R5295.
[33] S. Schuppler, N. Fischer, Th. Fauster, W. Steinmann, Appl. Phys. A 51 (1990) 322.
[34] I.L. Shumay, U. Höfer, Ch. Reuss, U. Thomann, W. Waller, Th. Fauster, Phys. Rev. B 58 (1998) 13974.
[35] Ch. Reuss, I.L. Shumay, U. Thomann, M. Kuschera, M. Weinelt, Th. Fauster, U. Höfer, Phys. Rev. Lett. 82 (1999) 153.
[36] S. Ogawa, H. Nagano, H. Petek, Phys. Rev. Lett. 78 (1997) 1339.
[37] U. Höfer, I.L. Shumay, Ch. Reuss, U. Thomann, W. Wallauer, Th. Fauster, Science 277 (1997) 1480.
[38] U. Höfer, Appl. Phys. B 68 (1999) 38.
[39] T. Fauster, Ch. Reuss, I.L. Shumay, M. Weinelt, Chem. Phys. 251 (2000) 111.
[40] E. Knoesel, A. Hotzel, M. Wolf, J. Electron. Spectrosc. Relat. Phenom. 88–91 (1998) 577.
[41] H. Ueba, Prog. Surf. Sci. 55 (1997) 115.
[42] P. Guyot-Sionnest, Phys. Rev. Lett. 66 (1991) 1489.
[43] J.C. Owrutsky, J.P. Culver, M. LI, Y.R. Kim, M.J. Sarisky, M.S. Yeganch, A.G. Yodh, R.M. Hochstrasser, J. Chem. Phys. 97 (1992) 4421.
[44] M. Bonn, Christian Hess, S. Funk, J.H. Miners, B.N.J. Persson, M. Wolf, G. Ertl, Phys. Rev. Lett. 84 (2000) 4653.
[45] M. Wolf, Surf. Sci. 377–379 (1997) 343.
[46] Electron Dynamics in Metals, Special issue of Chem. Phys. 251 (2000).
[47] M. Sargent III, M.O. Scully, W.E. Lamb Jr., Laser Physics, Addison-Wesley Pub. Co, London, 1974.
[48] R. Loudon, The Quantum Theory of Light, Oxford University Press, Oxford, 1973.
[49] J.C. Diels, W. Rudolph, Ultrashort Laser pulse Phenomena, Academic Press, San Diego, 1996.
[50] R.W. Schoenlein, J.G. Fujimoto, G.L. Eesley, T.W. Capehart, Phys. Rev. Lett. 61 (1988) 2596;
R.W. Schoenlein, J.G. Fujimoto, G.L. Eesley, T.W. Capehart, Phys. Rev. B 41 (1990) 5436;
R.W. Schoenlein, J.G. Fujimoto, G.L. Eesley, T.W. Capehart, Phys. Rev. B 43 (1991) 4688.

[51] S. Mukamel, Phys. Rev. A 28 (1983) 3480.
[52] T. Mii, H. Ueba, Surf. Sci. 427–428 (1999) 324.
[53] M. Bauer, S. Pawlik, M. Aeschlimann, Phys. Rev. B 60 (1999) 5016.
[54] T. Mii, H. Ueba, J. Lumin. 87–89 (2000) 898.
[55] H. Ueba, T. Mii, Appl. Phys. A 71 (2000) 537.
[56] K. Boger, M. Roth, M. Weinelt, T. Fauster, P.-G. Reinhard, Phys. Rev. B 65 (2002) 075104.
[57] M. Weinelt, Surf. Sci. 482–485 (2001) 519.
[58] H. Ueba, T. Sawabu, T. Mii, Surf. Sci. 502–503 (2002) 254.
[59] D. Gavoret, P. Nozières, B. Roulet, M. Combescot, J. Phys. (Paris) 30 (1969) 987.
[60] For review see P.M. Echenique, J.M. Pitarke, E.V. Chulkov, A. Rubio, Chem. Phys. 251 (2000) 1;
P.M. Echenique, R. Berndt, E.V. Chulkov, Th. Fauster, A. Goldman, U. Höfer, Surf. Sci. Rep. 52 (2004) 219, and references therein.
[61] B. Gumhalter, H. Petek, Surf. Sci. 445 (2000) 195;
B. Gumhalter, Surf. Sci. 518 (2002) 81.
[62] F. El-Shaer, B. Gumhalter, Phys. Rev. Lett. 93 (2004) 236804.
[63] M. Sakaue, H. Kasai, A. Okiji, J. Phys. Soc. Jpn 68 (1999) 720;
M. Sakaue, H. Kasai, A. Okiji, Jpn. J. Appl. Phys. 39 (2000) 4380;
M. Sakaue, H. Kasai, A. Okiji, Appl. Surf. Sci. 169 (2001) 68.
[64] M. Sakaue, T. Munakata, H. Kasai, A. Okiji, Phys. Rev. B 66 (2002) 094302;
M. Sakaue, T. Munakata, H. Kasai, A. Okiji, Phys. Rev. B 68 (2003) 205421;
M. Sakaue, T. Munakata, H. Kasai, A. Okiji, Surf. Sci. 532–535 (2003) 30.
[65] B. Gumhalter, Phys. Rev. B 72 (2005) 165406.
[66] P. Lazić, V.M. Silkin, E.P. Chulkov, P.M. Echenique, B. Gumhalter, Phys. Rev. Lett. 97 (2006) 086801.
[67] V.M. Silkin, J.M. Pitarke, E.V. Chulkov, P.M. Echenique, Phys. Rev. B 72 (2005) 115435.
[68] A. Peres, Am. J. Phys. 48 (1980) 931;
P. Facchi, H. Nakazato, S. Pascazio, Phys. Rev. Lett. 86 (2001) 2699.